Why and how pixels are becoming more and more intelligent (sensors – part 2)

Gian-Franco Dalla Betta

Department of Industrial Engineering, University of Trento and INFN
Via Sommarive 9, 38123 Povo di Trento (TN), Italy
gianfranco.dallabetta@unitn.it

2nd International Summer School on:
INtelligent Signal Processing for FrontIEr Research and Industry

July 14th-25th, 2014
Paris Diderot University, Paris

Outline

- Introduction
  - Radiation damage issues
- 3D and active edge sensors
- Charge multiplication
  - Avalanche based tracking sensors
- Conclusion

Introduction

- Radiation sensors are p-n junction devices
- Intelligence is normally on the ROC side …
- A few significant exceptions:
  - Silicon drift detector (E. Gatti, P. Rehak, 1983)
  - DEPFET (J. Kemmer, G. Lutz,1987)

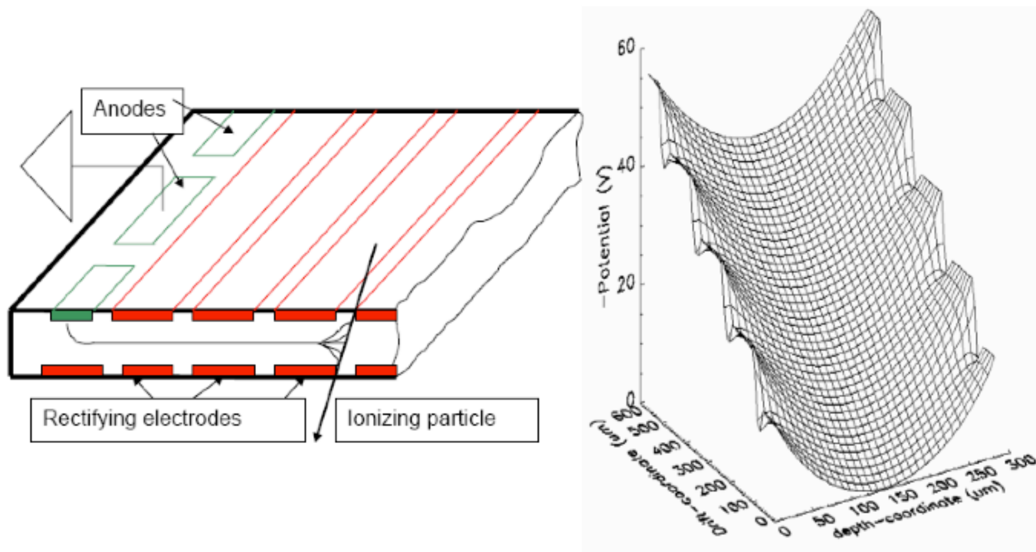

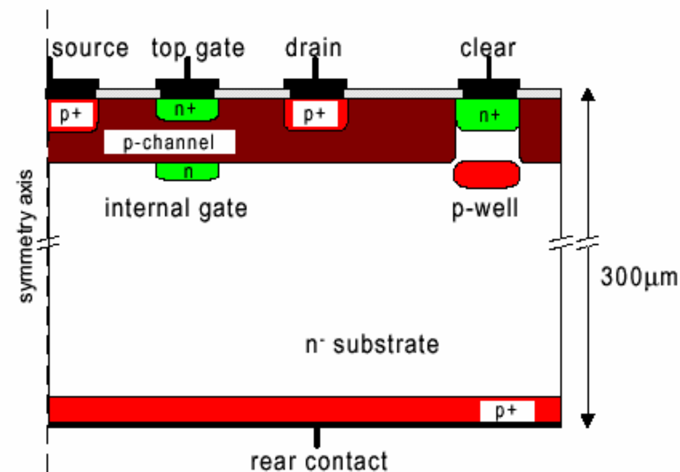

Bulk radiation damage in silicon sensors

Creation of deep-level defects

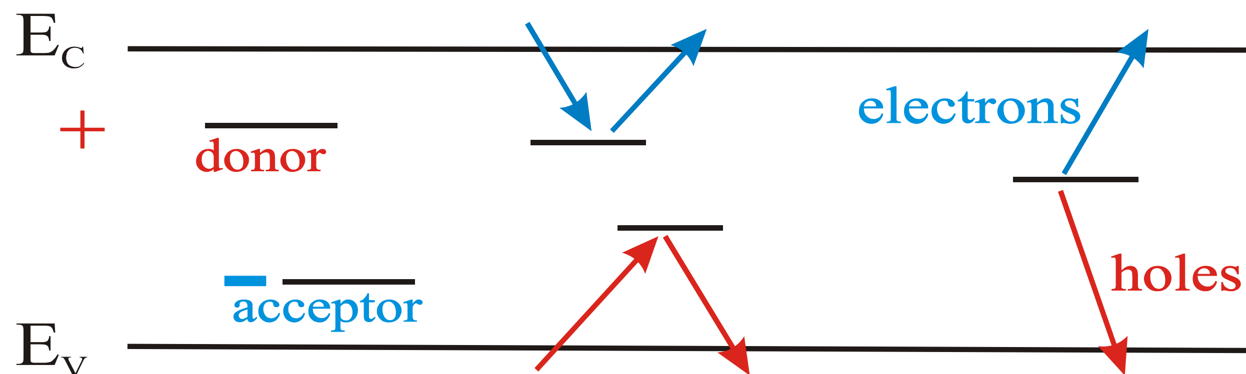

charged defects
⇒ **N_{eff} , V_{dep}**
e.g. donors in upper and acceptors in lower half of band gap

Trapping (e and h)
⇒ **CCE**
shallow defects do not contribute at room temperature due to fast detrapping

generation
⇒ **leakage current**
Levels close to midgap most effective

Shockley-Read-Hall statistics

Impact on detector properties can be calculated if all defect parameters are known:

$\sigma_{n,p}$: cross sections **E : energy level** **N_t : concentration**

Michael Moll – MC-PAD Network Training, Ljubljana, 27.9.2010

Radiation damage: macroscopic effects

1. Growth of leakage current

Growth of the shot noise component

Growth of power consumption (risk of thermal runaway)

2. Change of the effective doping concentration

1st stage increment of the bias voltage
2nd inability to provide the sufficient bias
=> partial depletion operation (less signal available)

3. Decrease of trapping time

loss of carriers during the drift
=> less signal available

4. Increase of silicon resistivity (upper limit is intrinsic silicon)

Radiation damage **Reduction of Signal/Noise**

Charge trapping and inter-electrode spacing

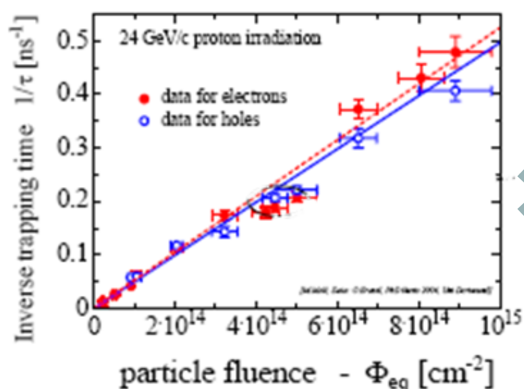

τ_{tr} Trapping Times

×

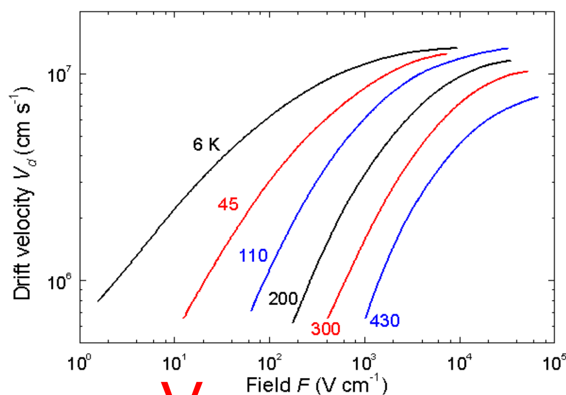

V_n Drift Velocity

=

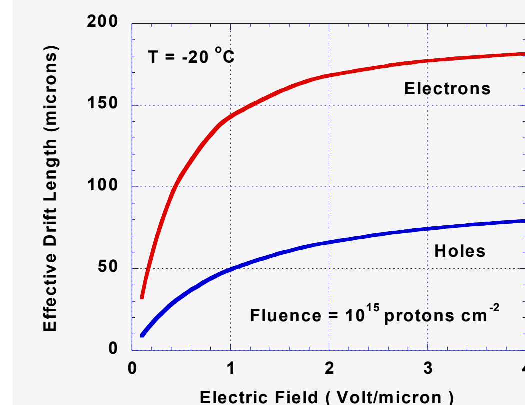

λ Effective drift length

$$\frac{dS}{dt} = q\frac{dV_W}{dx}\frac{dx}{dt}\exp(-\frac{x}{\lambda})$$

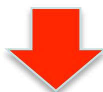

$$S = \frac{\lambda}{L}\left[1-\exp(-\frac{L}{\lambda})\right]$$

Expected signal efficiency after irradiation (without multiplication) depends on λ/L

$$SE = \frac{1}{1+0.6L\frac{K_\tau}{v_D}\Phi}$$

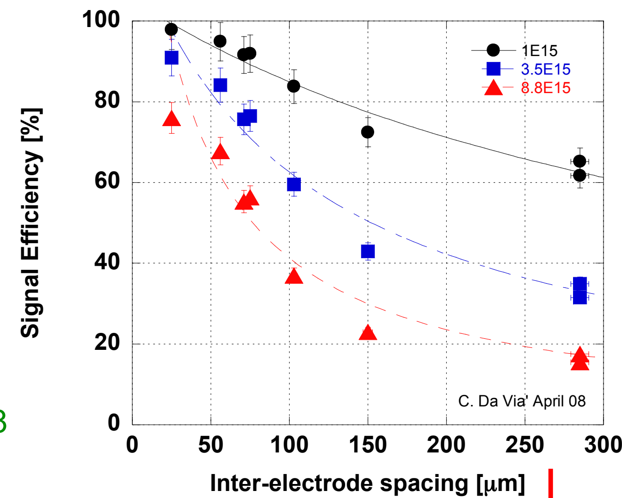

Trapping times from G. Kramberger et al, NIMA 481 (2002) 100, NIMA 501 (2003) 138

Calculations from C. Da Via, NIMA 603 (2009) 319

Outline

- Introduction
  - Radiation damage issues
- 3D and active edge sensors
- Charge multiplication
  - Avalanche based tracking sensors
- Conclusion

3D detectors

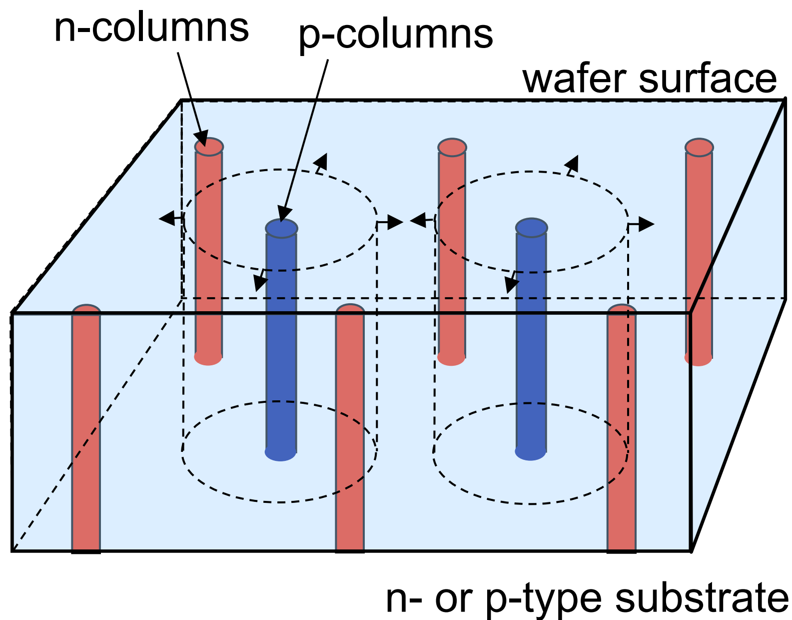

S. Parker et al. NIMA395 (1997)

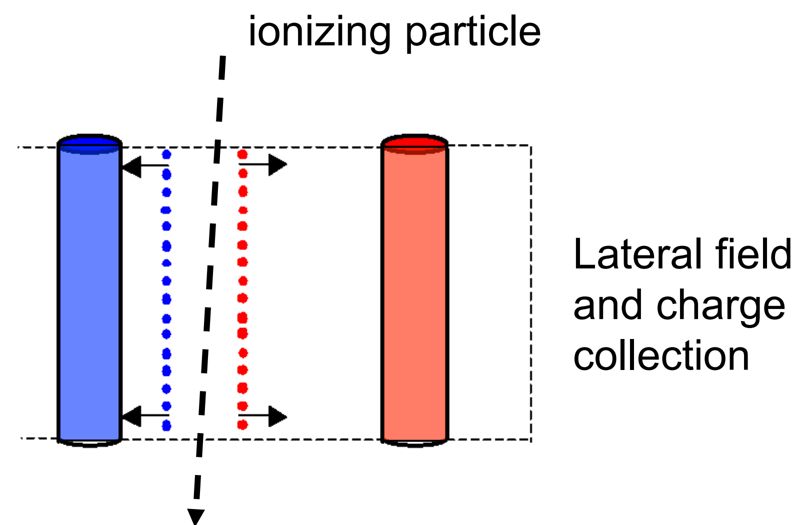

- Distance between *n* and p electrodes can be made short (~50 μm)

➡ extremely radiation hard detector

- First HEP application:
the ATLAS Insertable B-Layer (IBL)

C. Da Via et. al. NIMA 694 (2012), 321

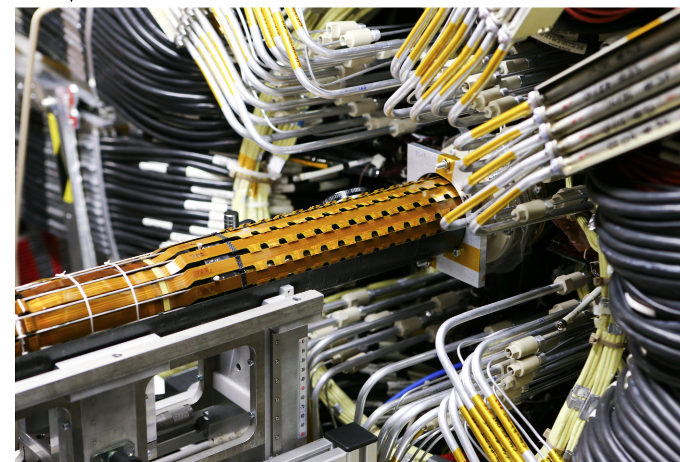

3D vs planar

Electrode distance (L) and active substrate thickness (Δ) are decoupled → L<<Δ by layout

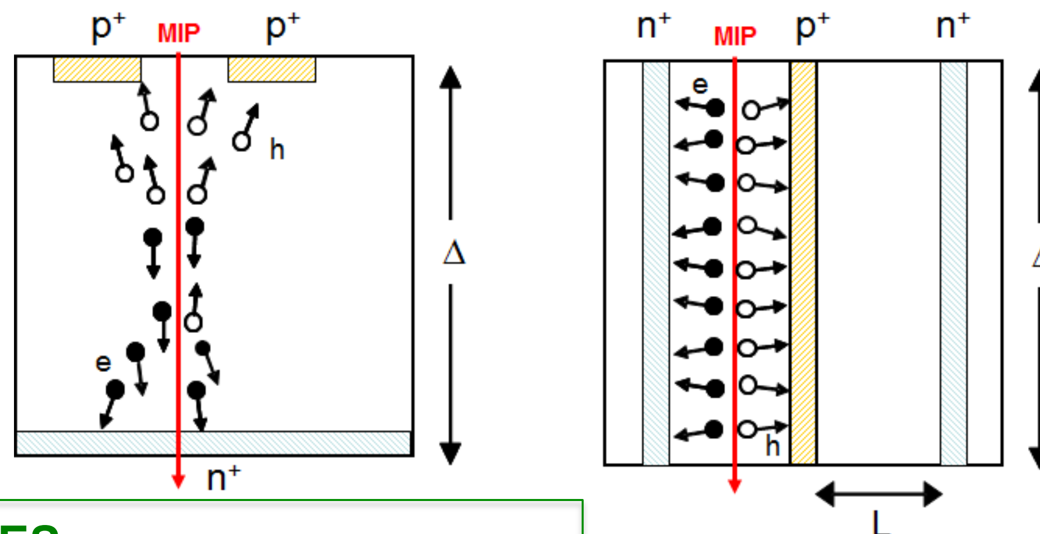

3D ADVANTAGES:

- Low depletion voltage (low power diss.)
- Short charge collection distance:
  - Fast response time
  - Less trapping probability after irr.
- Lateral drift → cell “shielding” effect:
  - Lower charge sharing
  - Low sensitivity to magnetic field
- **Active edges**

➡ **HIGH RADIATION HARDNESS**

DISADVANTAGES:

- Non uniform spatial response (electrodes and low field regions)
- Higher capacitance with respect to planar (~3-5x for ~ 200 μm thickness)
- Complicated technology (cost, yield)

Current, voltage, and power dissipation

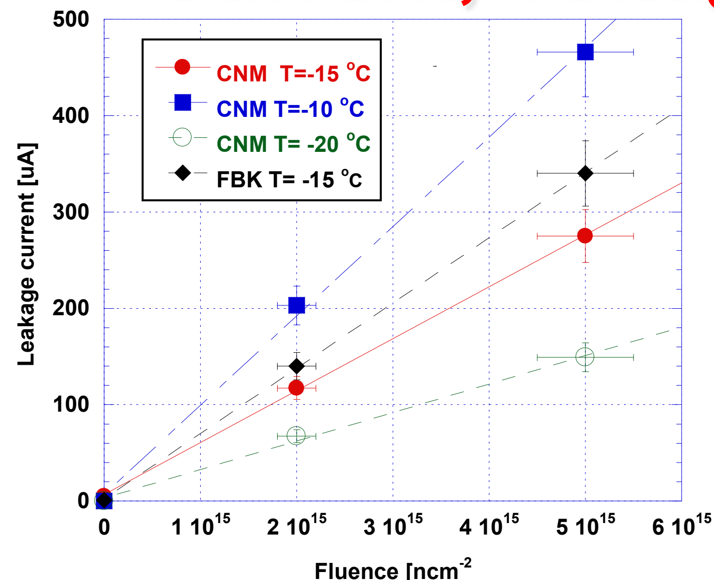

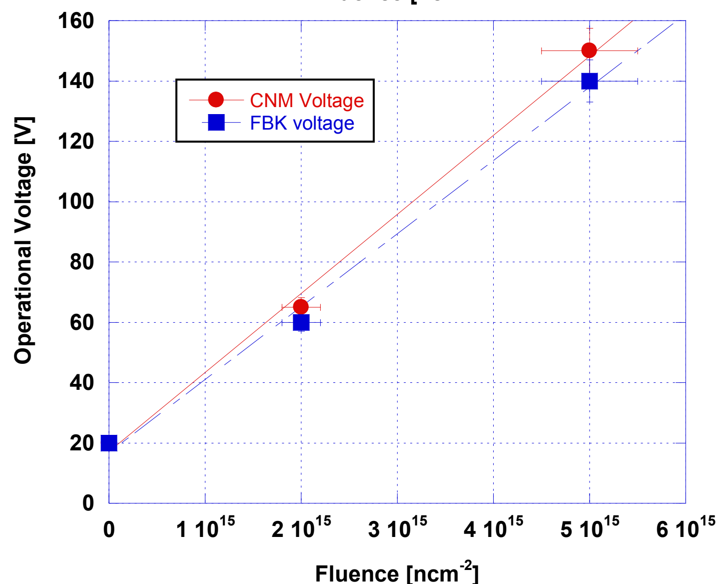

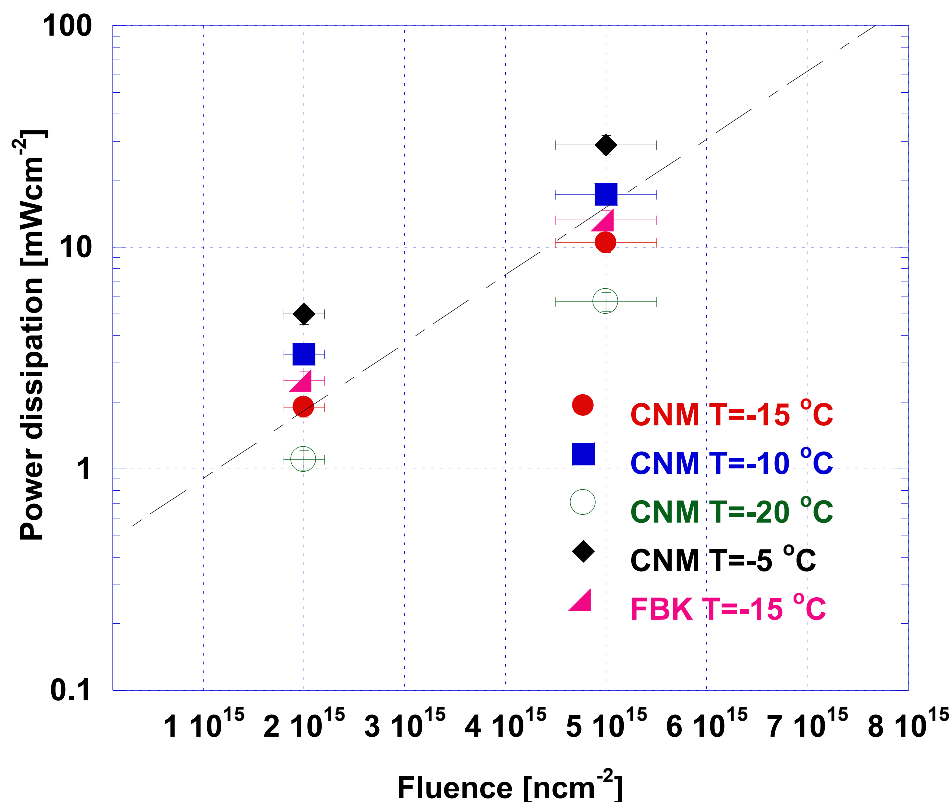

- ATLAS IBL requirement on sensor power dissipation < 200 mW/cm^2 at 5 x 10^{15} n$_{eq}$/cm^2 and -15 °C (after annealing)
- ~10X safety margin …

C. Da Via, C. Gemme, A. Micelli, S. Grinstein

Charge collection properties

Data from: ATLAS IBL Collaboration, JINST 7 (2012) P1101
+ S. Grinstein, unpublished results (FBK09)

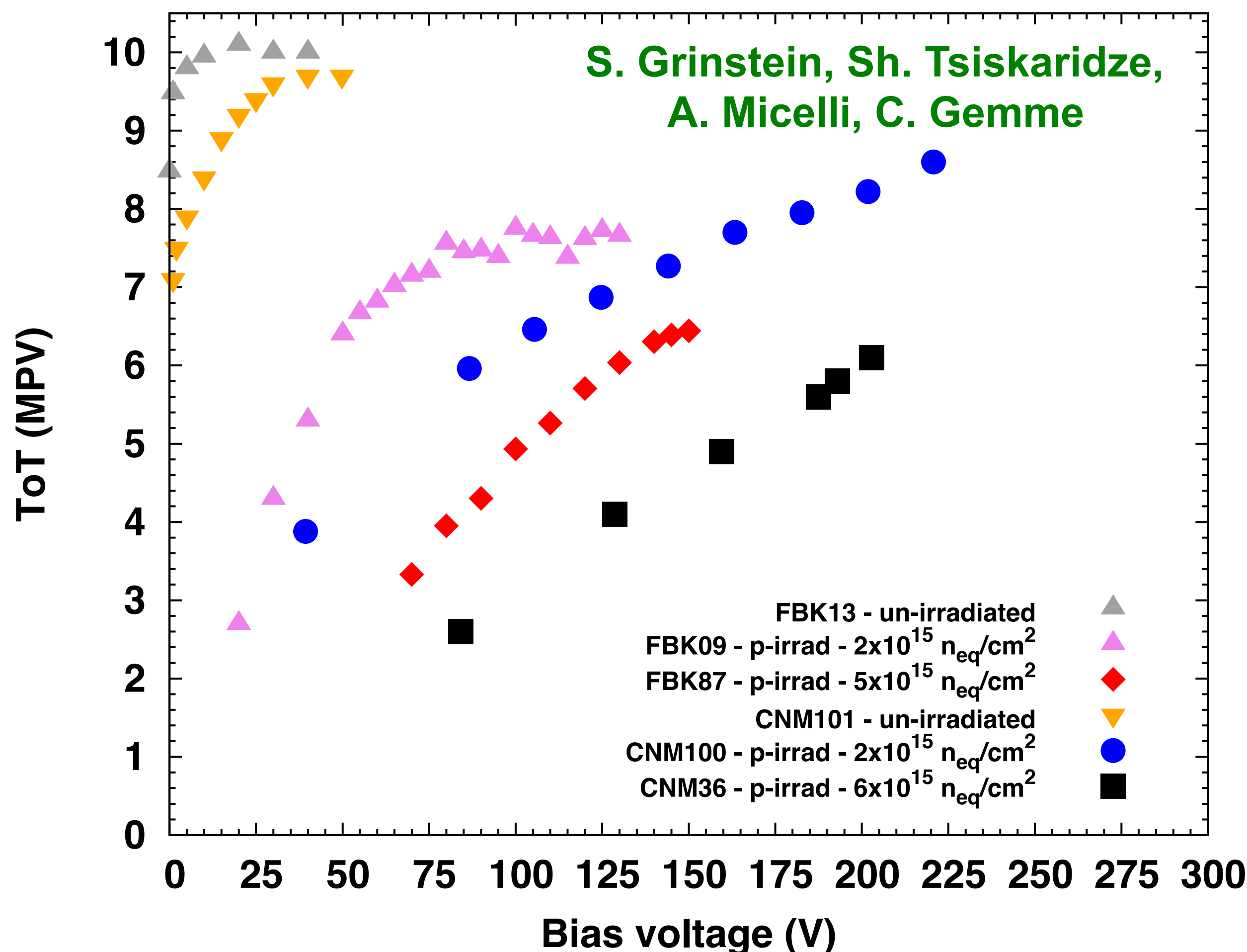

Irradiated 3D

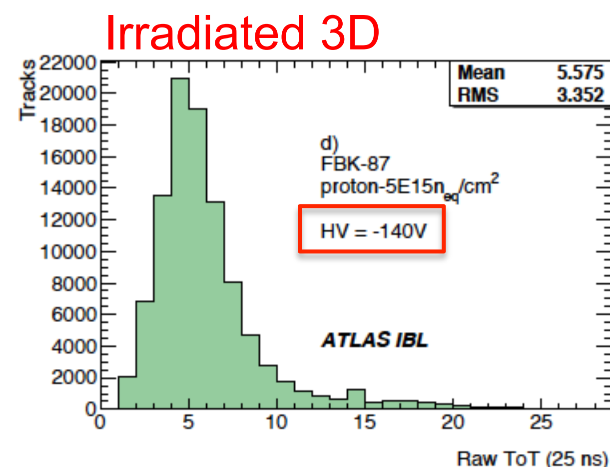

Irradiated planar

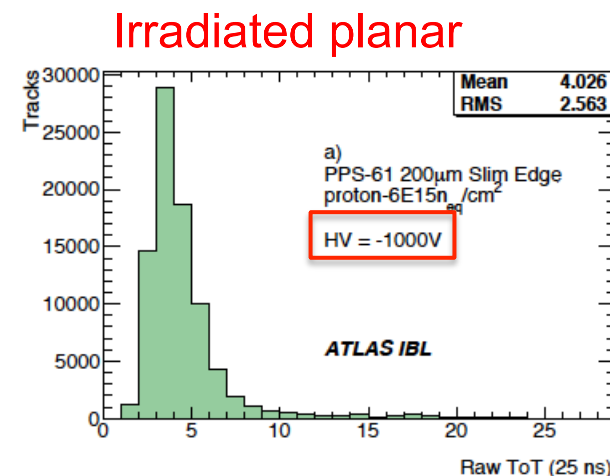

Speed

Best choice: trenched detectors

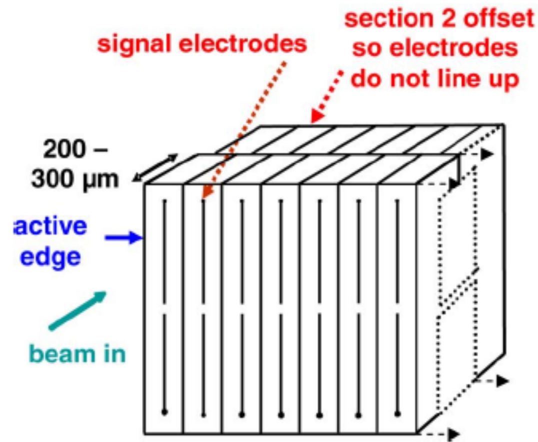

So far tested with hex-cell 3D's (L=50µm) & fast current amplifier

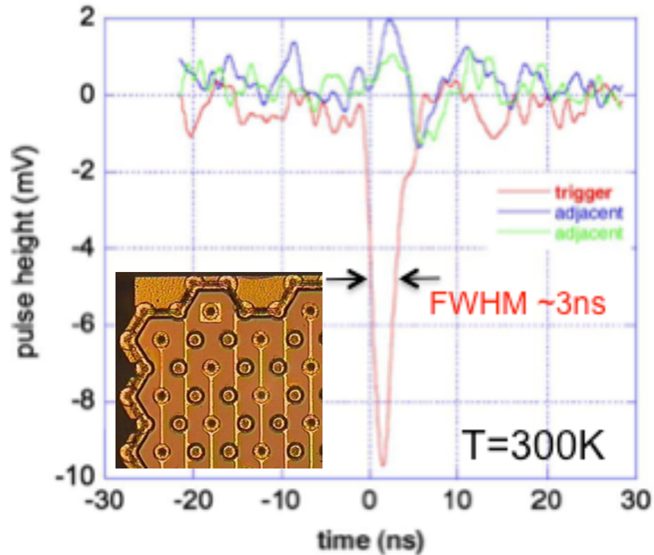

S. Parker et al. IEEE TNS 58(2) (2011) 404

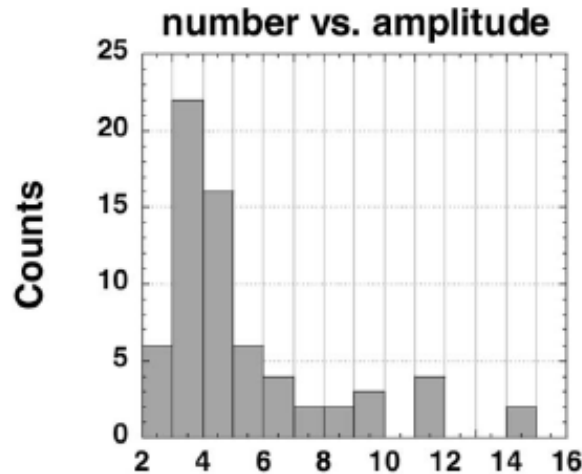

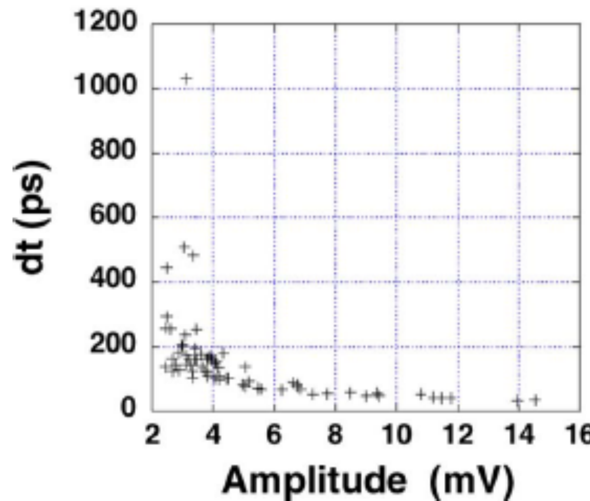

- Off-line analysis of recorded waveforms
- Timing resolution from 177 ps to 31ps
- Limited by front-end noise

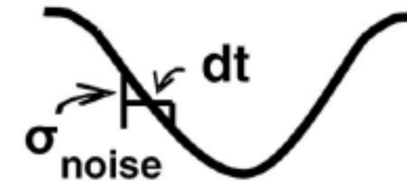

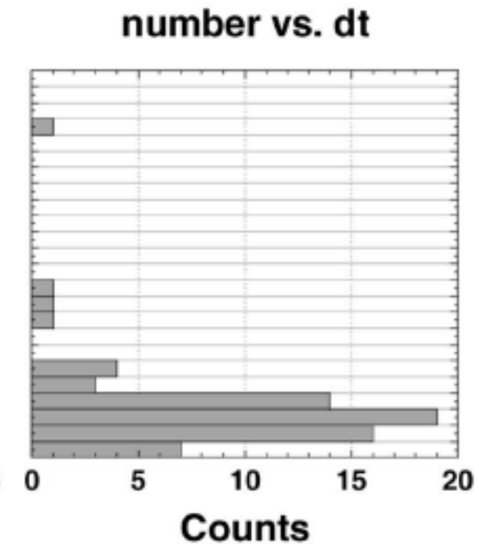

Capacitance and noise

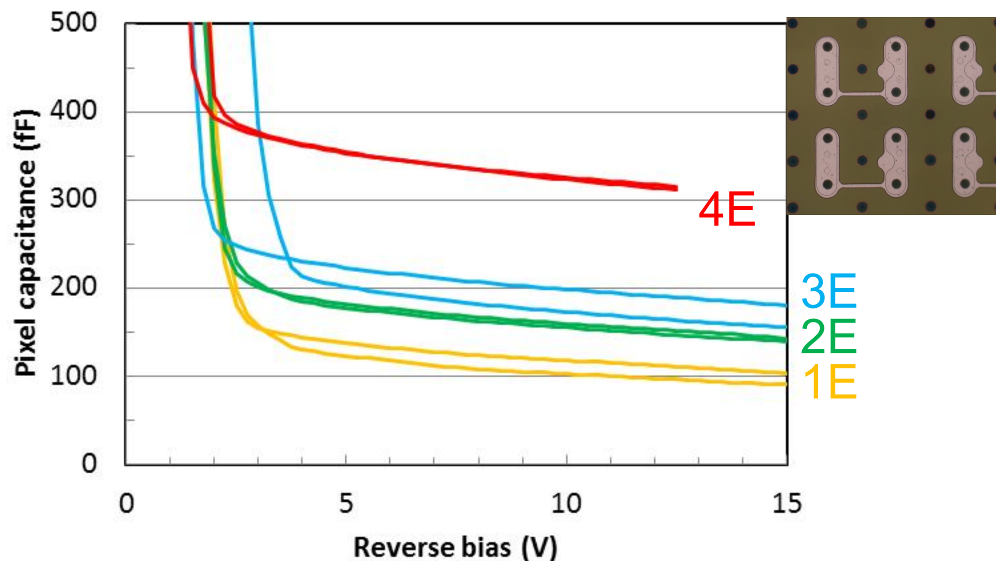

C. Da Via et al. NIMA 604 (2009) 505

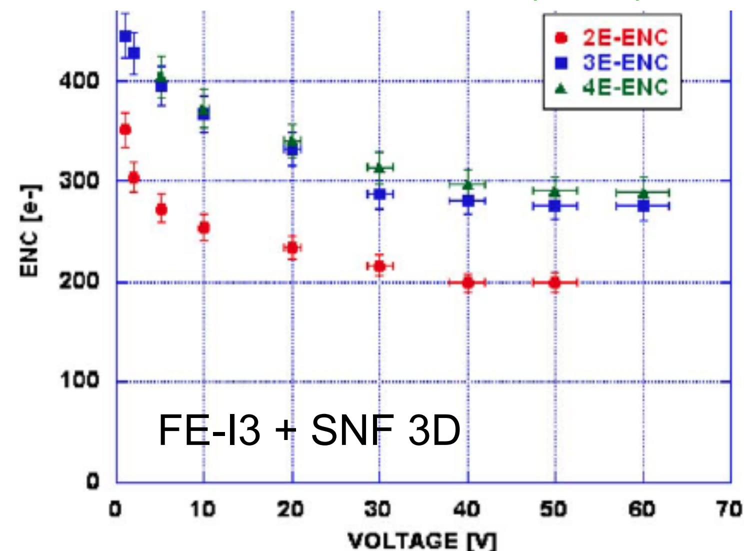

E. Alagoz et al. JINST 7 (2012) P08023

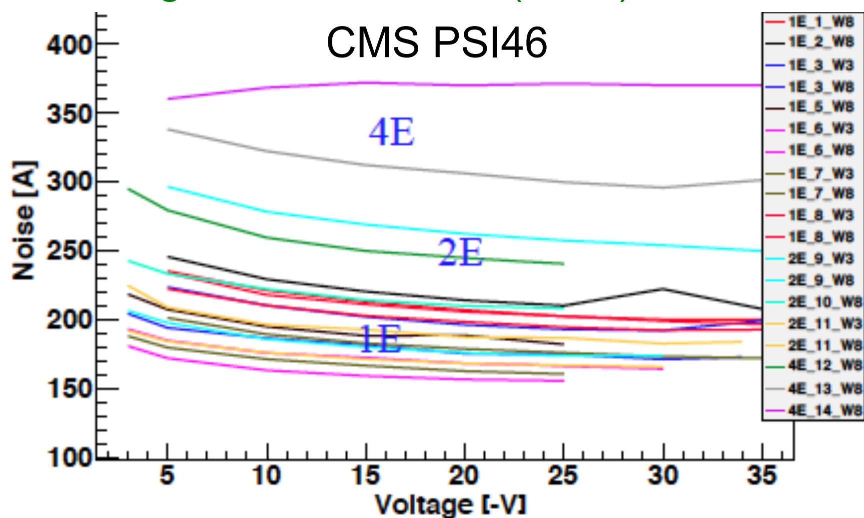

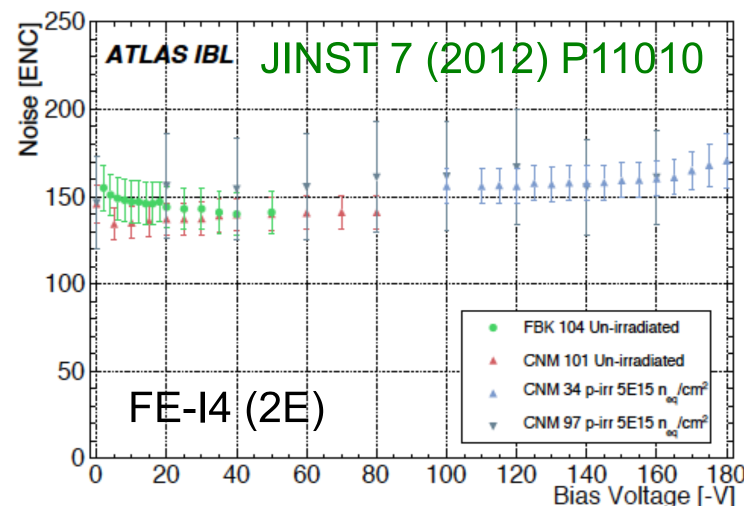

Null field points and delayed signals

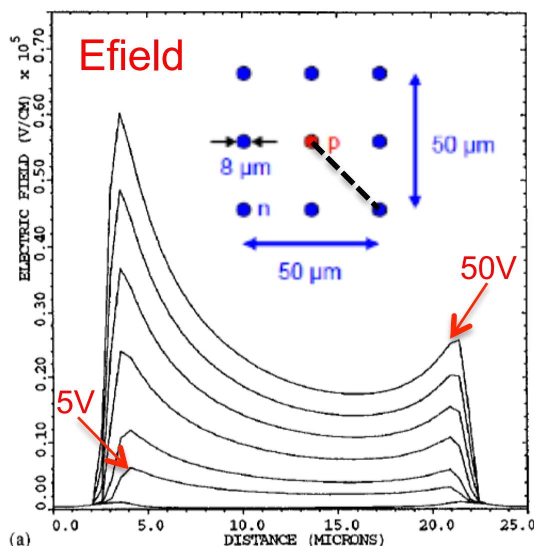

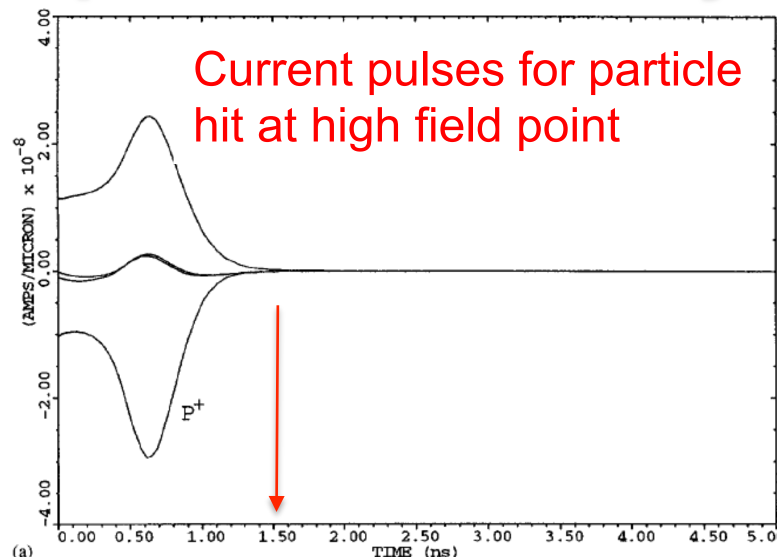

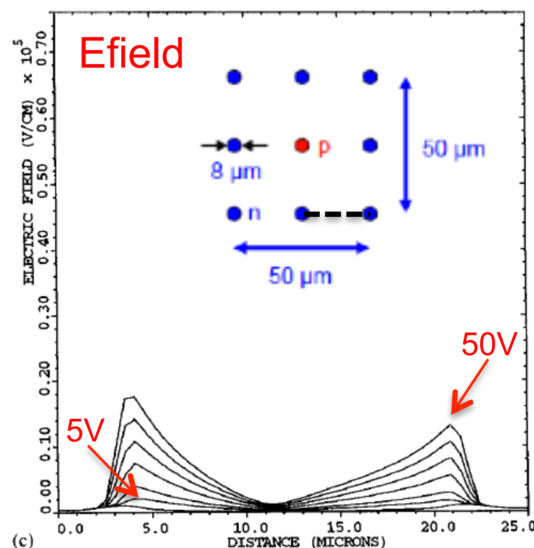

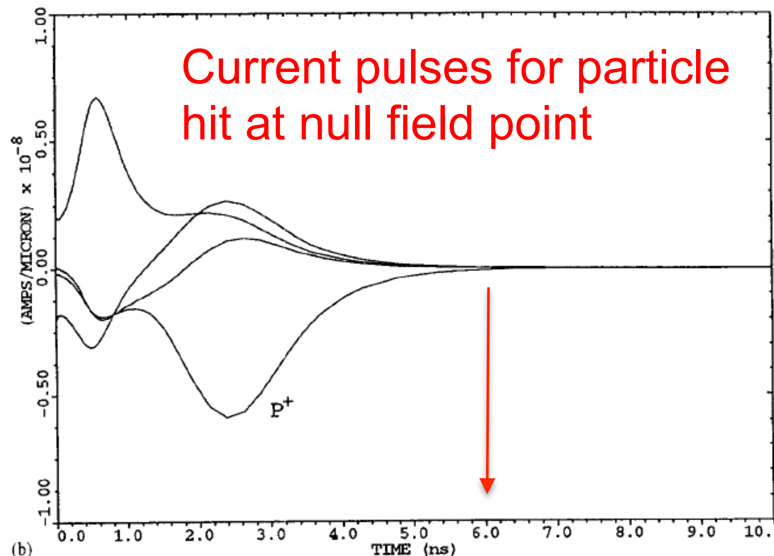

S. Parker et al. NIMA395 (1997) 328

- 3D structure implies null field points in between columnar electrodes of the same doping type
- Carriers generated at null field points first have to diffuse before drifting, thus delaying signals
- This can be improved with trenched electrodes, but at the expense of higher capacitance and reduced geometrical efficiency

Poly-Si electrode inefficiency

J. Hasi, PhD thesis, Brunel, 2004

Electrode response using 12 keV X-ray beam (ALS at LBNL), beam size ~ 2μm

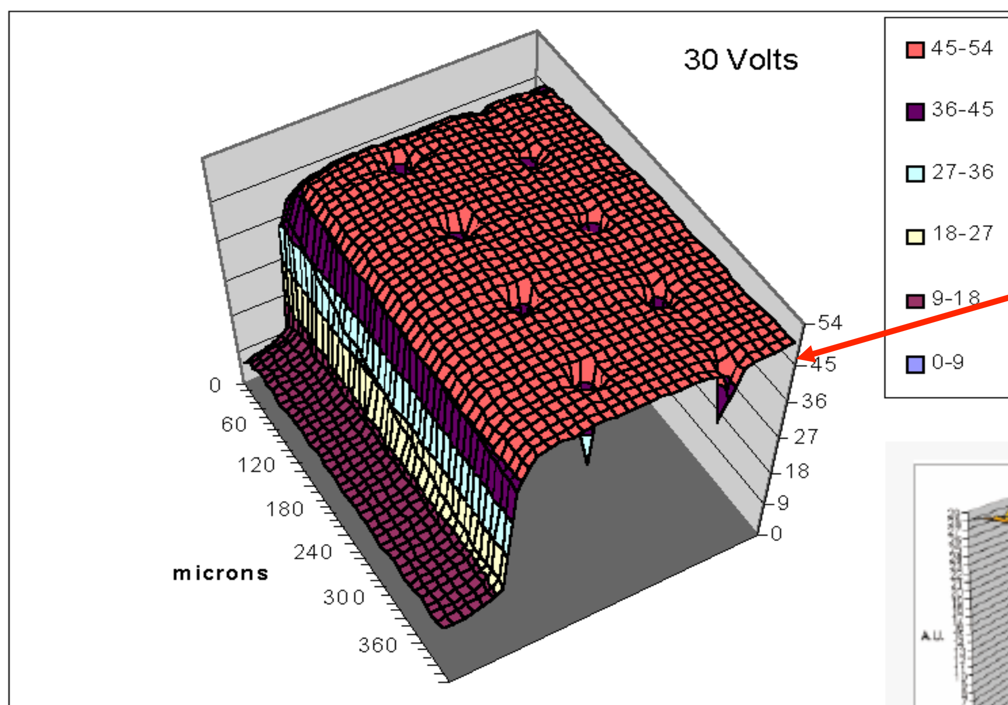

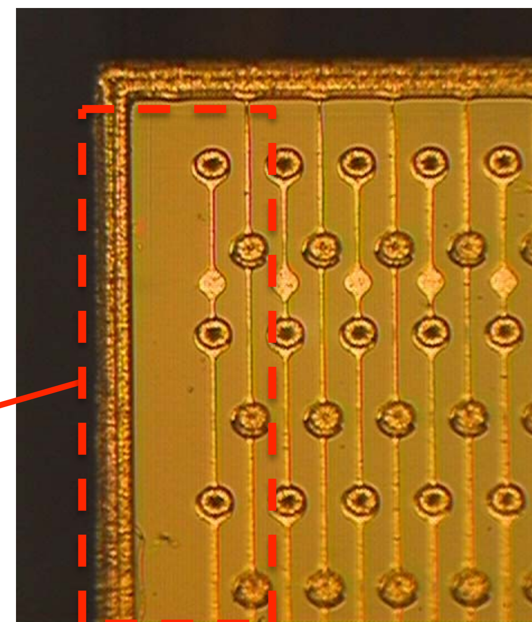

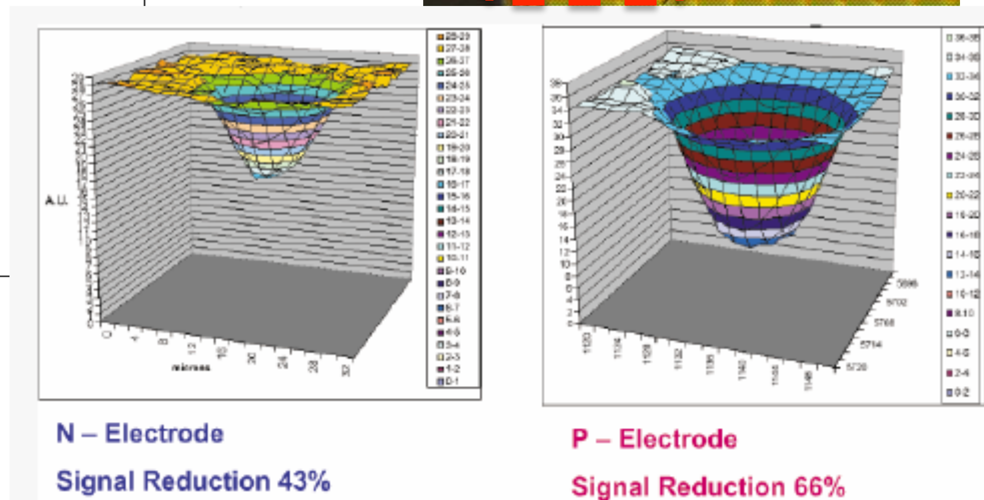

- Diffusion, lifetimes (poly-Si grain sizes)
- Oxide barrier effect at the interfaces …

→ Replace $POCl_3$ with PH_3

→ Replace BBr_3/O_2 with B_2H_6

Key technology: DRIE by the Bosch process

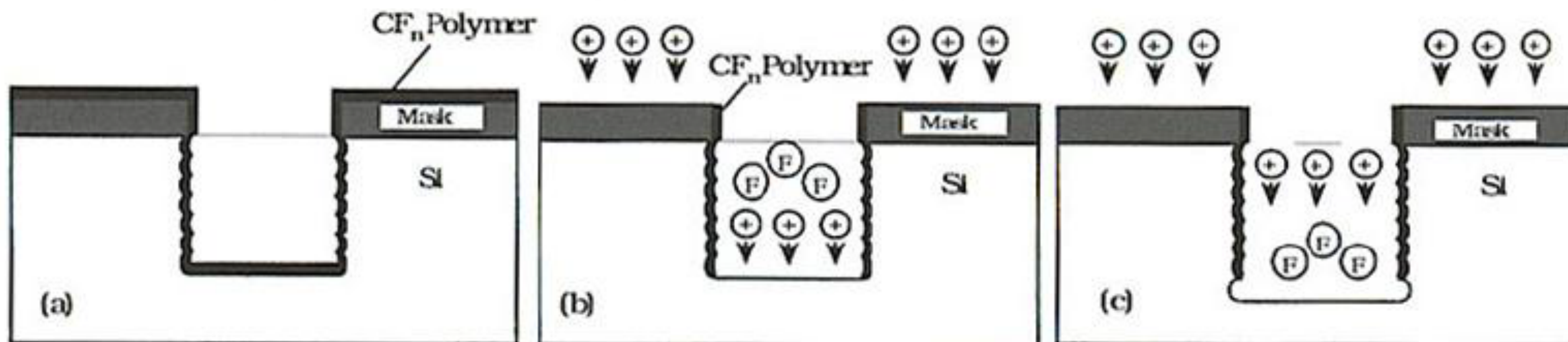

- Alternating etch cycles (SF_6) and passivation cycles (C_4F_8)
- High aspect ratio (~20:1 or better for trenches) and good uniformity

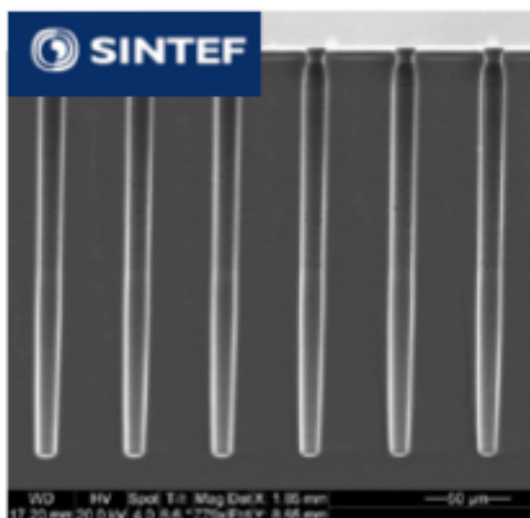

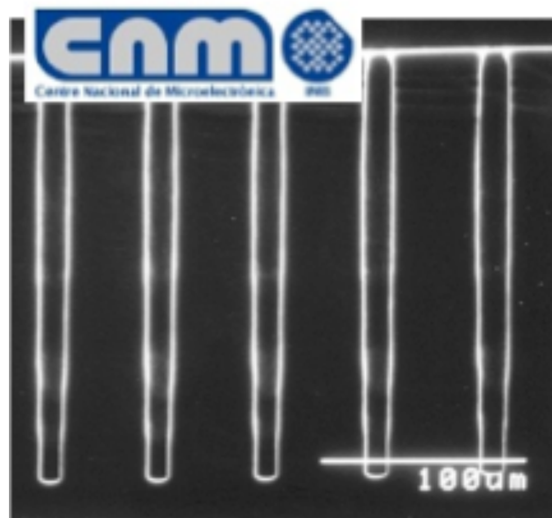

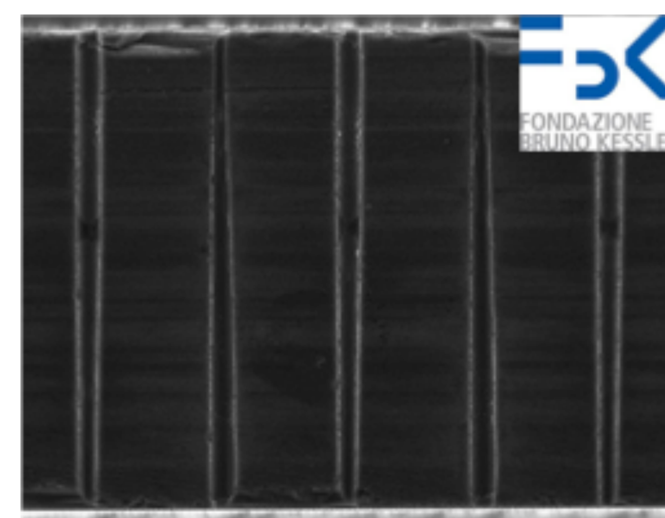

Full 3D with active edge

C. Kenney et al., IEEE TNS, vol. 46, n. 4 (1999) 1224
T.E. Hansen et al., JINST 4 (2009) P03010

detector wafer
oxide
support wafer

1) wafer bonding

resist

2) n+ hole definition and etching

n+ polysilicon

3) hole doping and filling

resist

4) p+ hole definition and etching

p+ polysilicon

5) hole doping and filling

metal

6) Metal deposition and definition

The sensor edge termination problem

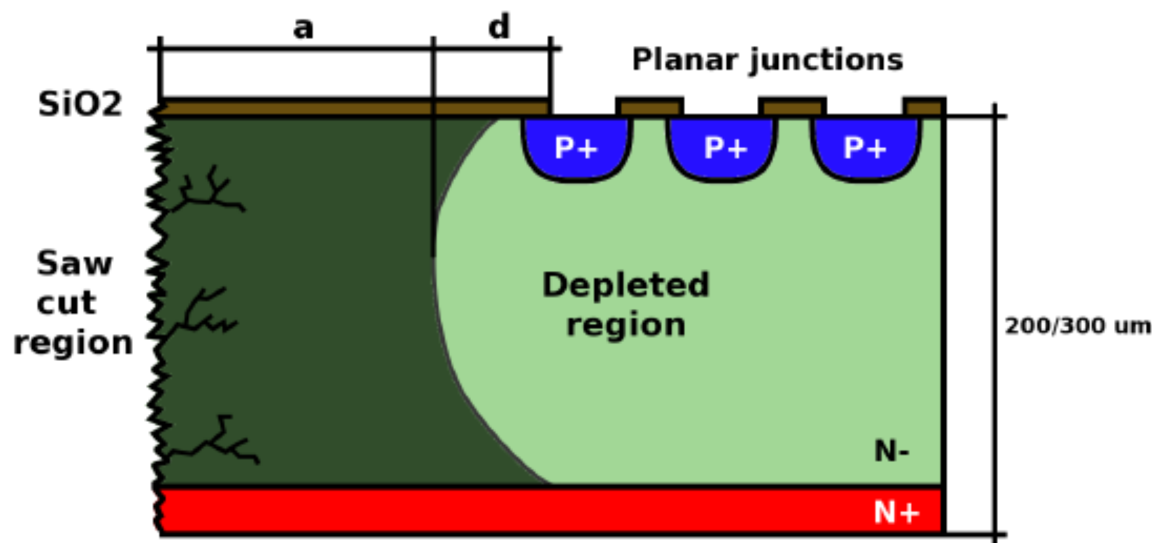

- In standard designs with saw-cut dicing, there's risk of high leakage current injection from the damaged cut region.
- Need to account for:

- Lateral depletion region (d)

- Additional safety margin (a), also used to host multiple guard rings in most designs for higher V_{bd} and better stability

➡ Wide dead area at the edge: a+d ~ 0.5 – 1 mm

Going edgeless

- Future HEP experiments (e.g. HL-LHC), due to material budget restrictions and tight mechanical constraints, call for new sensors for the inner layers (pixels) with reduced geometrical inefficiency, a trend that has already started with the ATLAS IBL
- TOTEM experiment uses 1-side edgeless strip sensors; other forward physics experiments (AFP,PPS) will use 1-side edgeless pixels

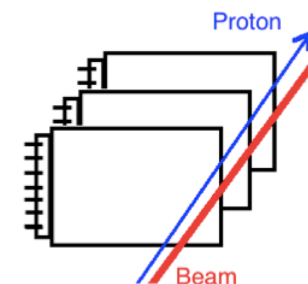

220m to ATLAS P1

- 4-side edgeless sensors are fundamental for X-ray imaging, so as to obtain seamless large area images by tiling the detectors into matrices
- 1-side edgeless sensors largely improves efficiency for X-ray imaging in the edge-on configuration

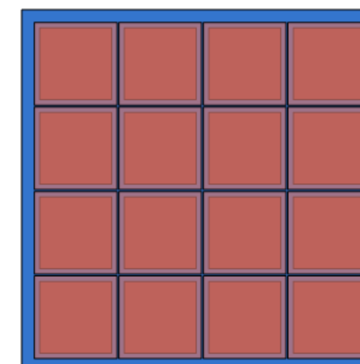

A major break-through: active edge

- First introduced at Stanford as an extension of 3D sensor technology, later applied also to planar sensors
- Cut lines are not sawed but etched with DRIE & doped

to act as electrodes, arbitrary shapes possible

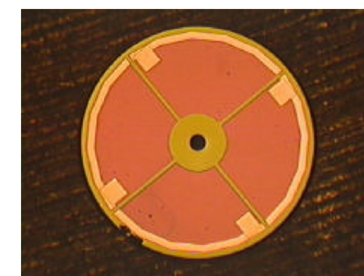

- Process is of course more complicated:
  - Need of support wafer → wafer bonding and final removal
  - Several DRIE steps (3-4 for 3D, 2 for planar)

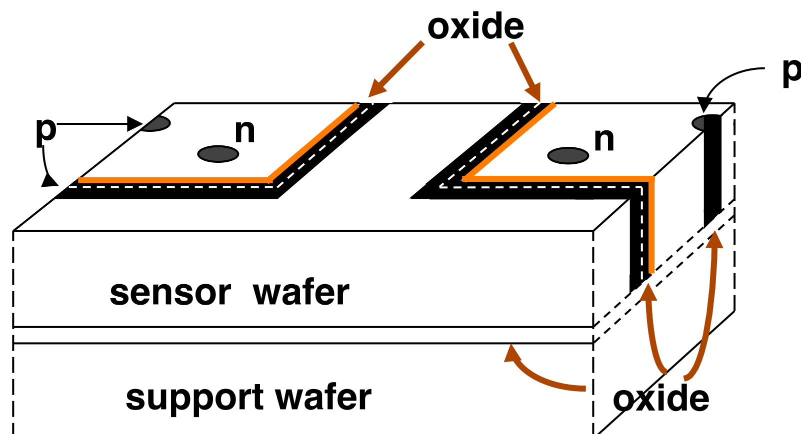

C. Kenney et al., IEEE TNS 48 (2001) 2405

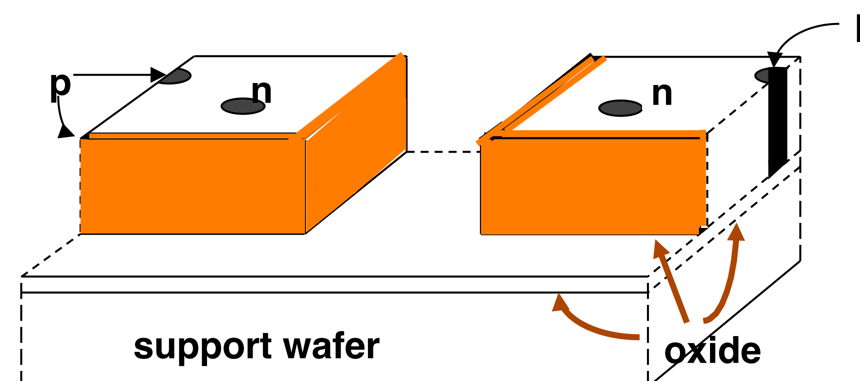

C. Kenney et al., NIMA 565 (2006) 272

Active edge: sensitivity

Planar active-edge strip sensors tested with 12.5 keV X-ray beam (FWHM 2 μm) at the Advanced Light Source (LBL)

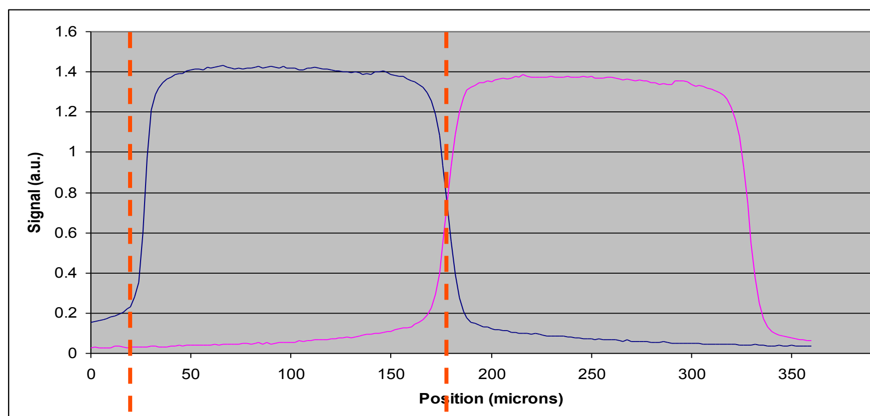

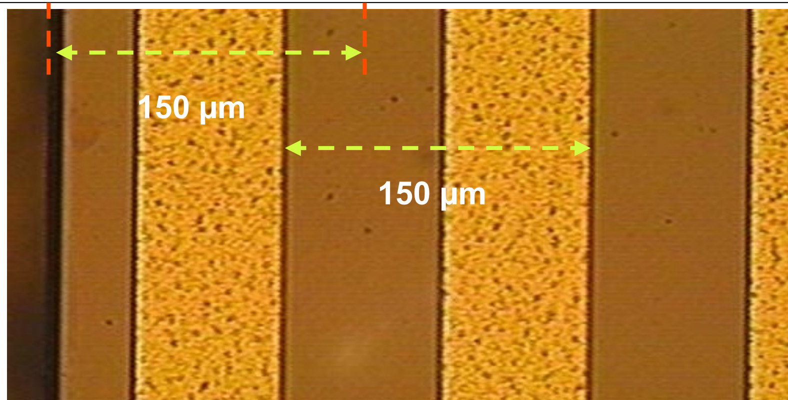

C. Kenney et al., NIMA 582 (2007) 178

3D active-edge pixel sensors coupled to FEI3 and tested with a 180 GeV/c pion beam at CERN

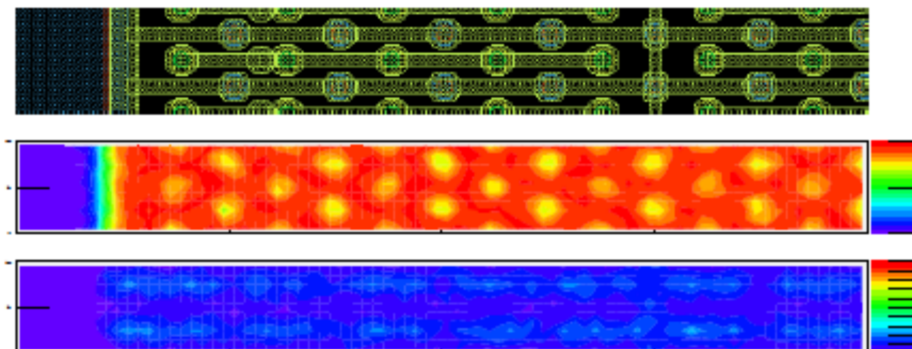

Hit efficiency projection onto the horizontal axis

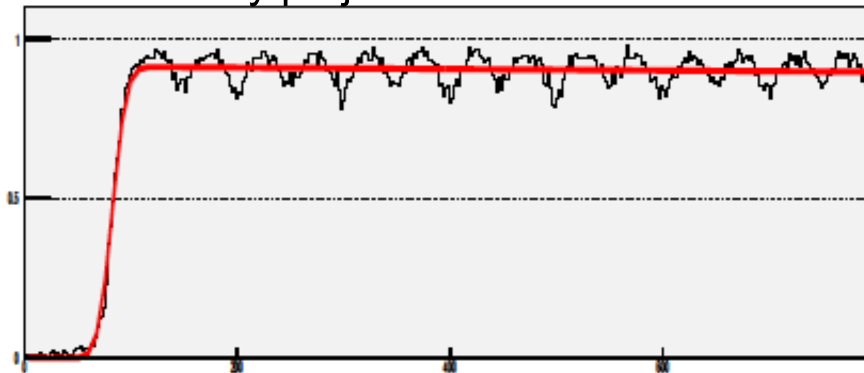

O. Røhne, IEEE NSS 2008, N27-8
C. Da Via, et al. IEEE TNS 56(2) (2009) 505

Active edge: recent highlights

Active edge technology now available also at other processing facilities (e.g., VTT, SINTEF, FBK).

VTT sensor with 4-quadrant edge implant

X. Wu et al., JINST 7 (2012) P02001

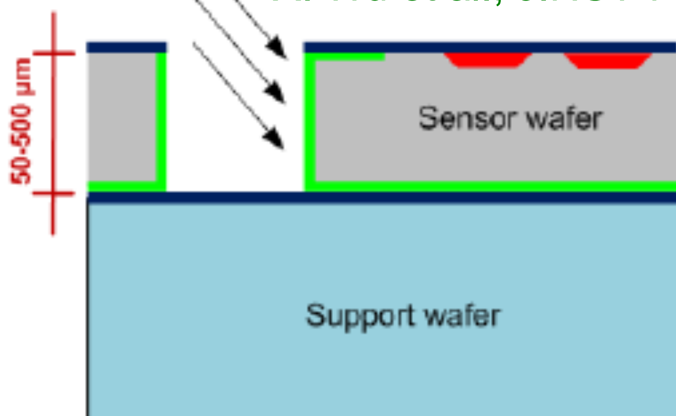

WIDEPIX 10x10 (http://www.widepix.cz)

J. Jakubek et al.,JINST 9 (2014) C04018

A. Macchiolo et al., HSTD9 (2013)

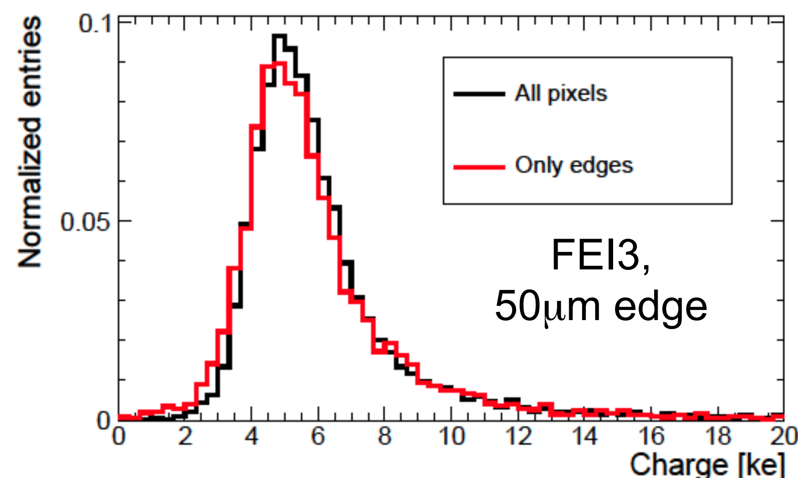

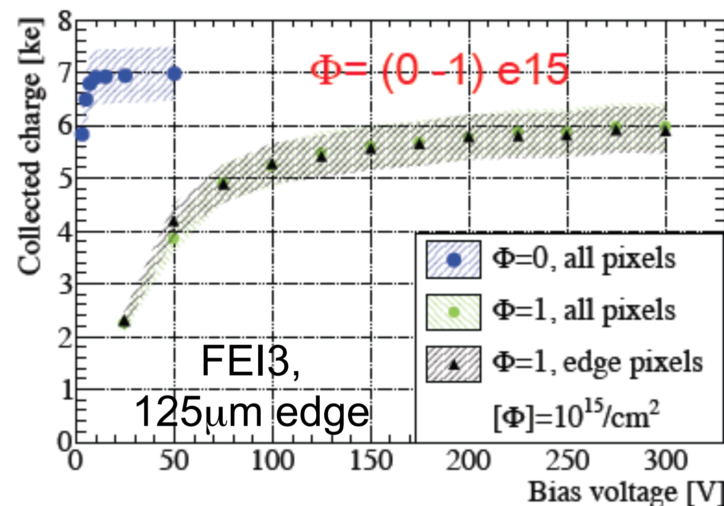

Double-sided 3D sensors

FBK (Trento, Italy)

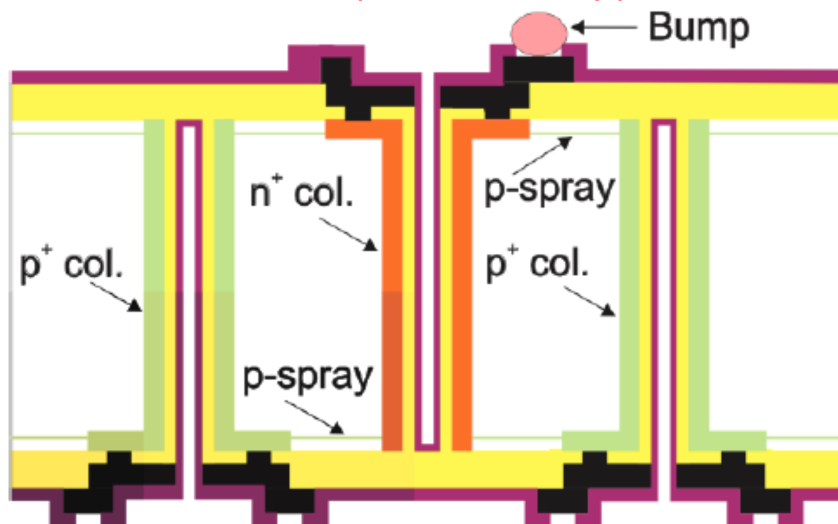

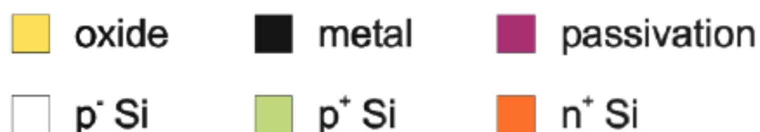

CNM (Barcelona, Spain)

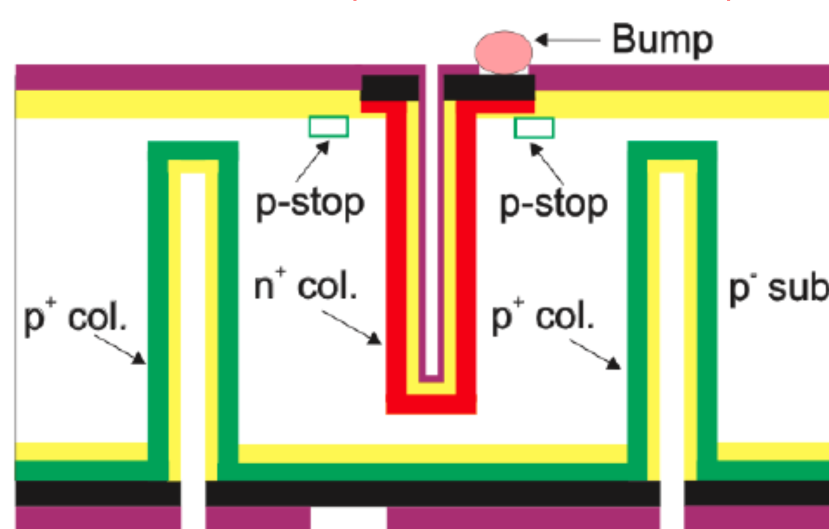

A. Zoboli et. al., IEEE TNS 55(5) (2008), 2775
G. Giacomini, et al., IEEE TNS 60(3) (2013) 2357

G. Pellegrini et. al. NIMA 592(2008), 38
G. Pellegrini et. al. NIMA 699(2013), 27

- Do not use support wafer → reduced process complexity
- Back-side accessible → Easier assembly within systems
- Active edge not feasible → Slim edge …

} Technology of choice for the IBL

Performance comparison

Signal Efficiency [%]

100, 80, 60, 40, 20, 0

0, 5 10^15, 1 10^16, 1.5 10^16, 2 10^16, 2.5 10^16

Fluence [ncm^-2]

55-100V -20C

FE-I4 pixel readout 200 µm or 230 µm column overlap [1]

FBK [4]

FBK

CNM

Stanford

160V 0C

140-160V -20C

Stanford 210 µm -diode [3]

200V -30C

~6000e- for 230µm column overlap

CNM 215 µm column overlap - microstrip readout [2]

C. Da Via' Feb. 2012

Signal Efficiency = Ratio of max. signal after irradiation and before irradiation

$$SE = \frac{1}{1 + K_C \cdot \Phi}$$

See slide 6

[1] ATLAS IBL Collaboration, JINST 7 (2012) P11010
[2] M. Koehler et al. NIMA 659 (2011) 272
[3] C. Da Via, et al., NIMA 604 (2009) 505
[4] G.-F. Dalla Betta, et al., HSTD9 (2013)

Original Compilation by C. Da Via

Slim edge in FBK 3D sensors

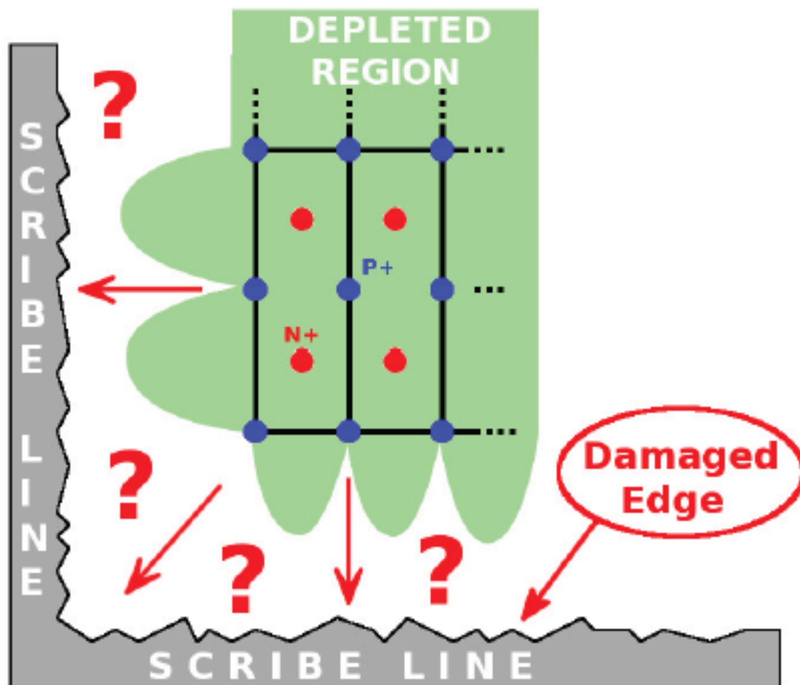

Layout, simulation and laser map

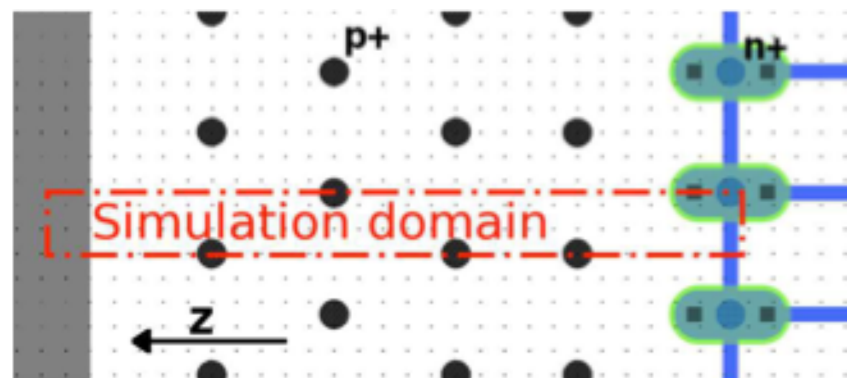

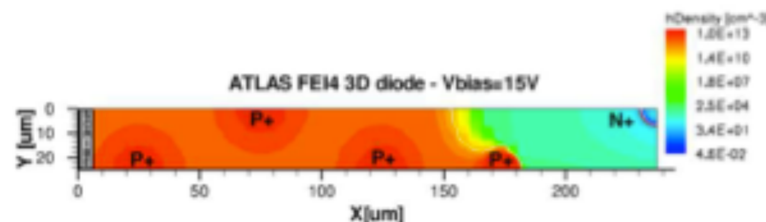

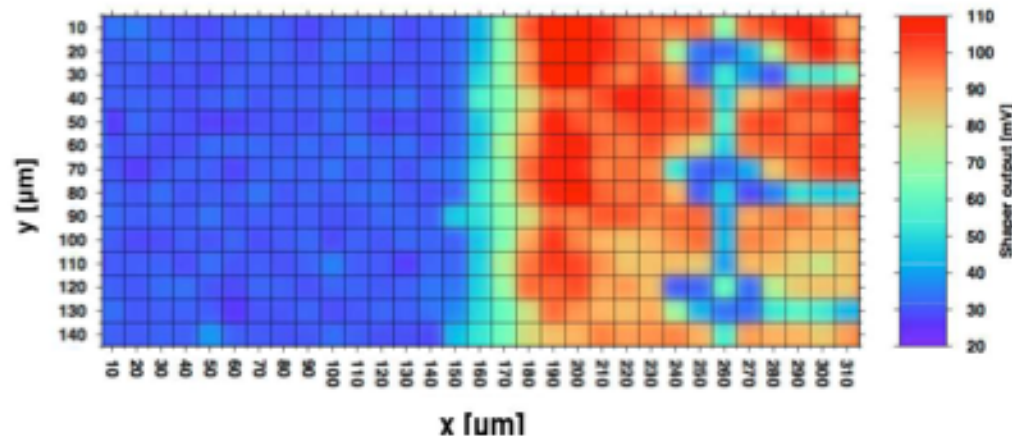

- Diamond saw cut still needed
- How to reduce the dead area ?
- Terminating structures ?
  (e.g., 3D guard ring at CNM)
- Multiple fence of ohmic columns …

M. Povoli, et al. JINST 7 (2012) C01015

Room for improvement …

M. Povoli, et al. JINST 7 (2012) C01015

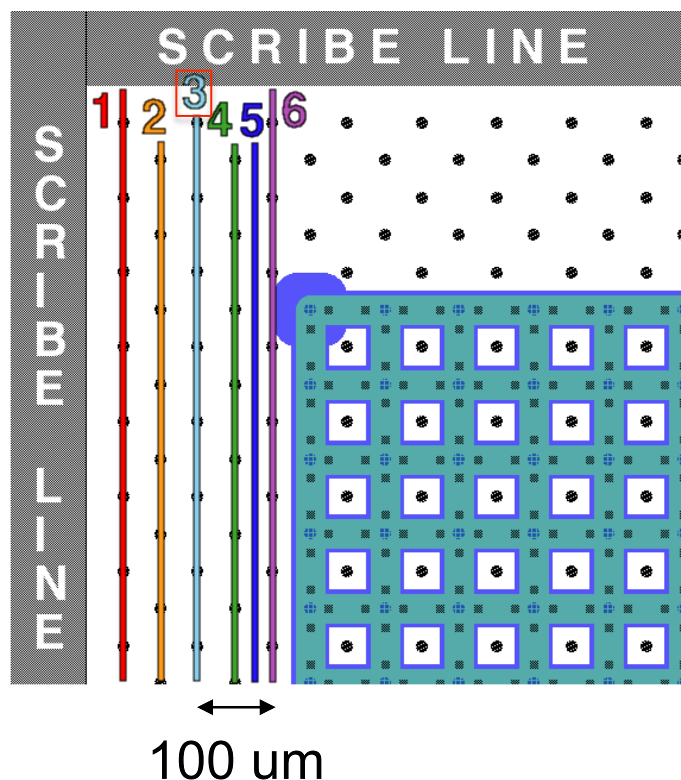

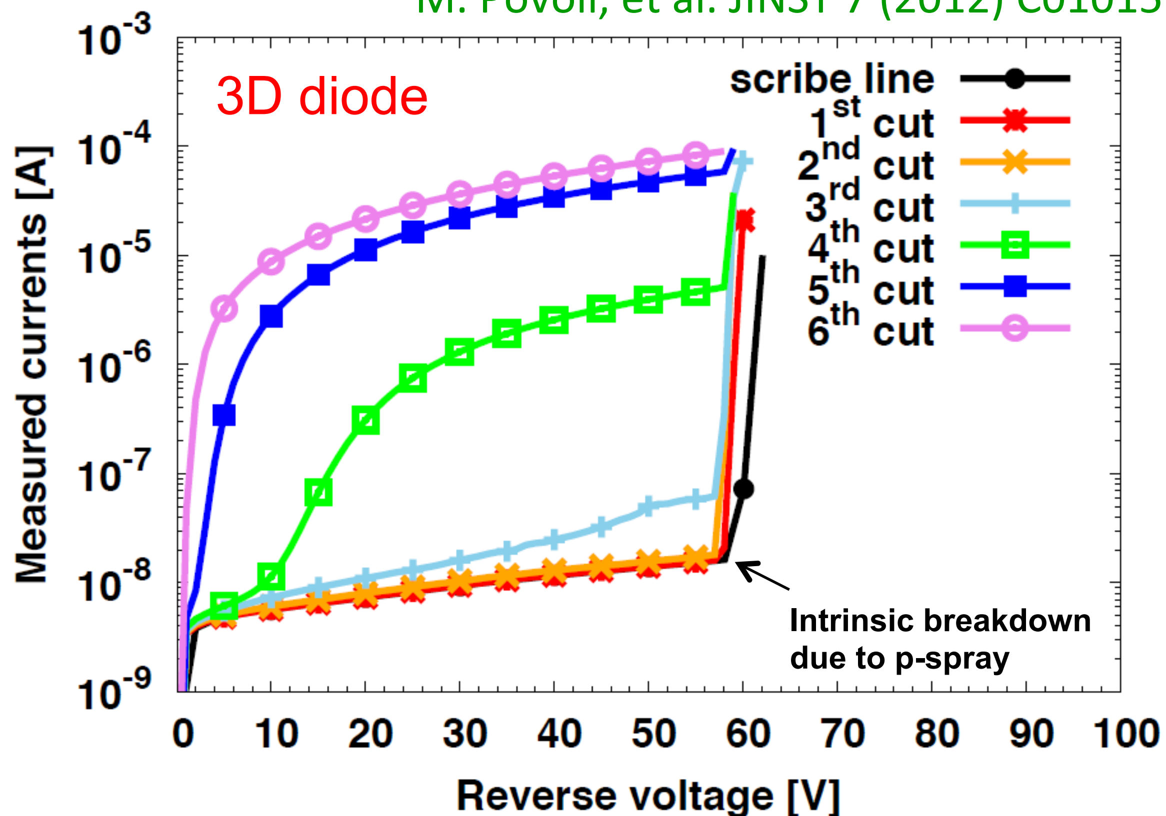

- Repeated cuts starting from scribe-line, each one closer to the active area (the 6th cut dices the last row of ohmic columns of the active area)
- Devices can be safely operated up to the 3rd cut (i.e., with only one row of ohmic columns beyond the active area)

  → There's room for design optimization (dead region ~ 100 μm)

Pixel Roadmap LHC → HL-LHC

N. Wermes, TN workshop 2014 in Genova

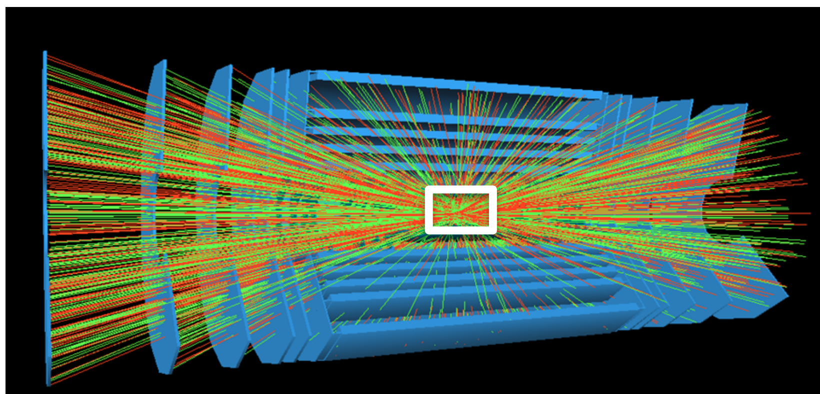

Technology roadmap →
5x Chip Size
½ threshold
20x TID dose
20x NIEL
6x event pile-up

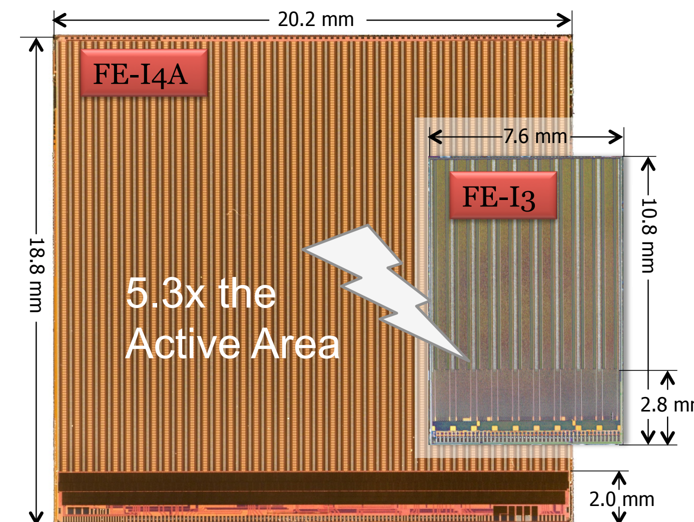

Increased luminosity requires:

- Higher hit-rate capability
- Increased granularity (e.g., 100x25 or 50x50 μm^2 pixel size)
- Higher radiation tolerance (up to a fluence of 2×10^{16} n_{eq} cm^{-2})
- Reduced material budget and better geometrical efficiency

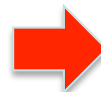

Implications for 3D sensors

- thinner sensors (back to SS approach with support wafer)
- narrower electrodes
- reduced electrode spacing
- very slim (or active) edges

3D pixels are an option for the innermost layers

Outline

- Introduction
  - Radiation damage issues
- 3D and active edge sensors
- Charge multiplication
  - Avalanche based tracking sensors
- Conclusion

What about planar sensors ?

- R&D on planar sensors has never stopped. In particular, CERN RD48 and then RD50 have deeply investigated:
  - Different substrates (oxygen enriched FZ, MCz, epitaxial, …) and non-Si semiconductors
  - Low temperature operation
  - Forward bias
  - Different configurations

    (from p-on-n to n-on-n to n-on-p)

http://www.cern.ch/rd50

- In 2008, first evidence of an unexpected effect, charge multiplication …

Charge multiplication in heavily irradiated Si sensors

Several groups have independently reported on strip or pad sensors with CCE larger than expected or even exceeding 100% …

J. Lange et. al., NIMA 624 (2010) 405

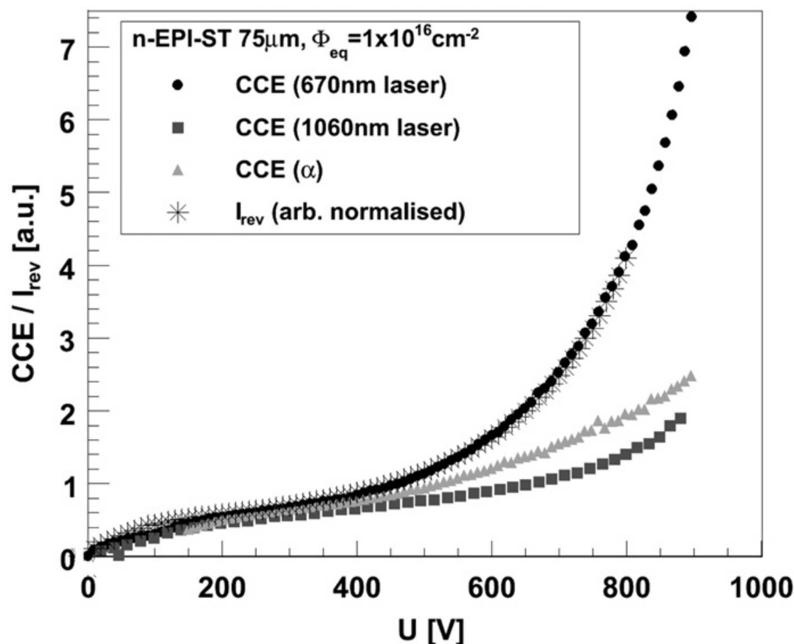

G. Casse et al., IEEE TNS 56 (2009) 3752

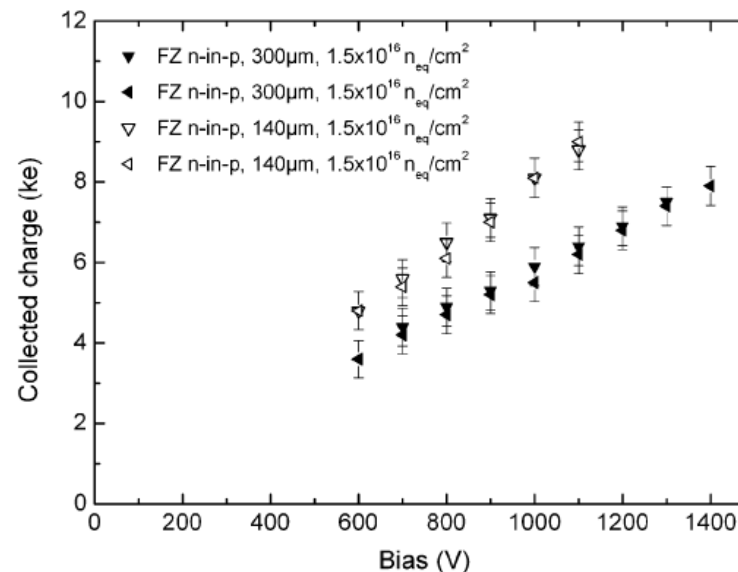

I. Mandic et al., NIMA 612 (2010) 474

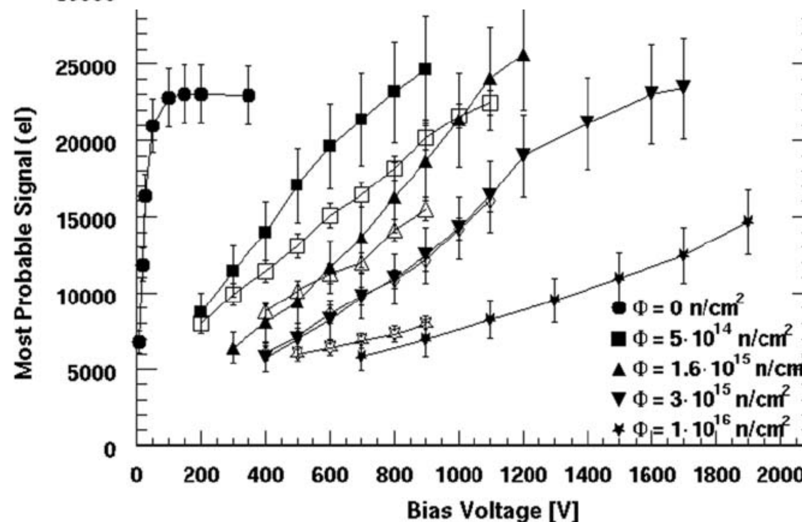

Open issues with charge multiplication

- Comprehensive modeling (edge-TCT gives deep insight)
- Long term stability
- System issues (HV, power)
- Control by modified design

G. Kramberger 15th RD50 Workshop, 2009

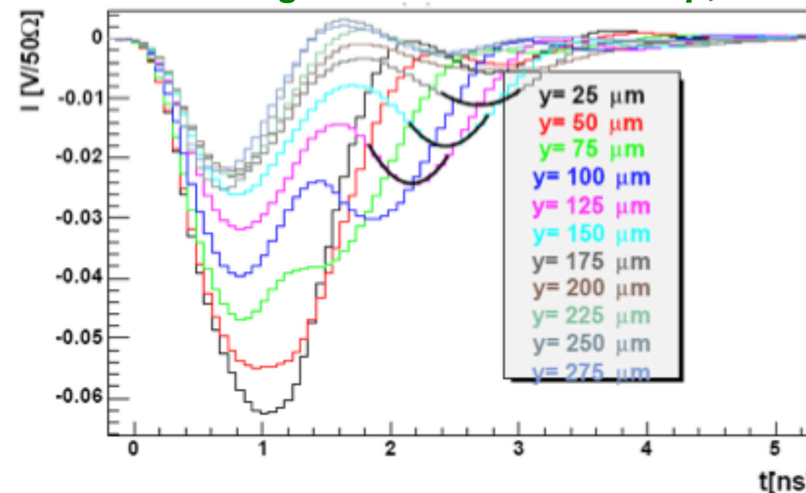

U. Parzefall, 24th RD50 Workshop, 2014

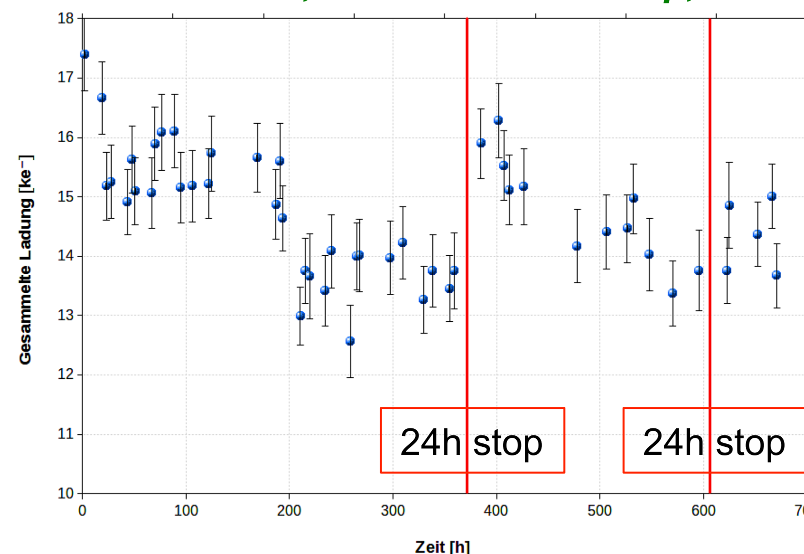

G. Casse et al NIMA 699(2013) 9.

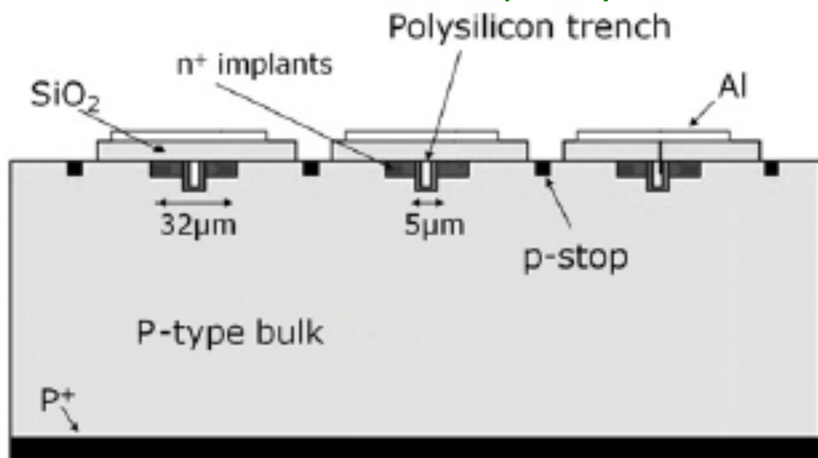

Impact ionization in reverse biased diode

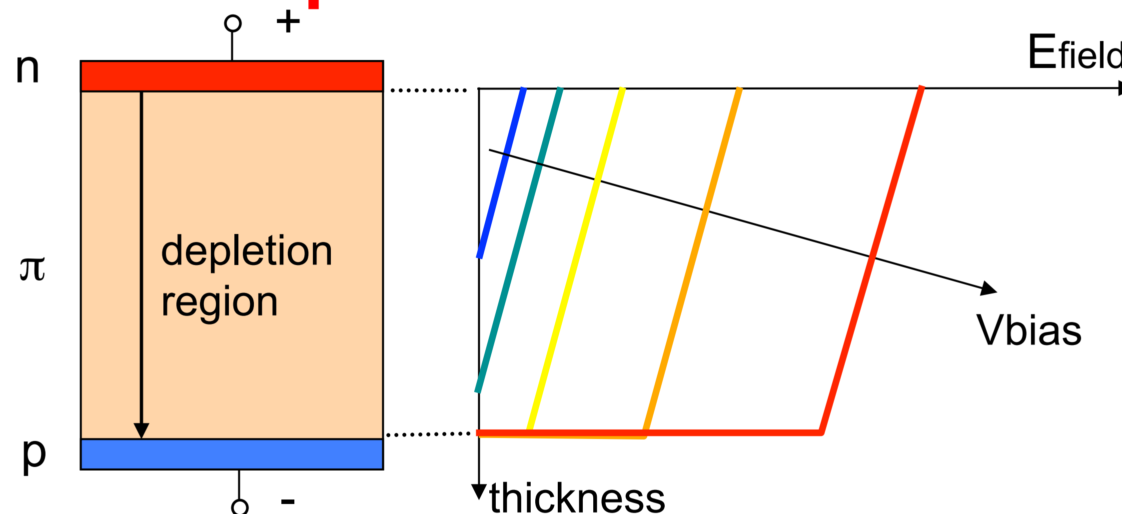

Impact ionization:
carriers have enough kinetic energy to break a bond, i.e.,
to move an electron from valence band to conduction band

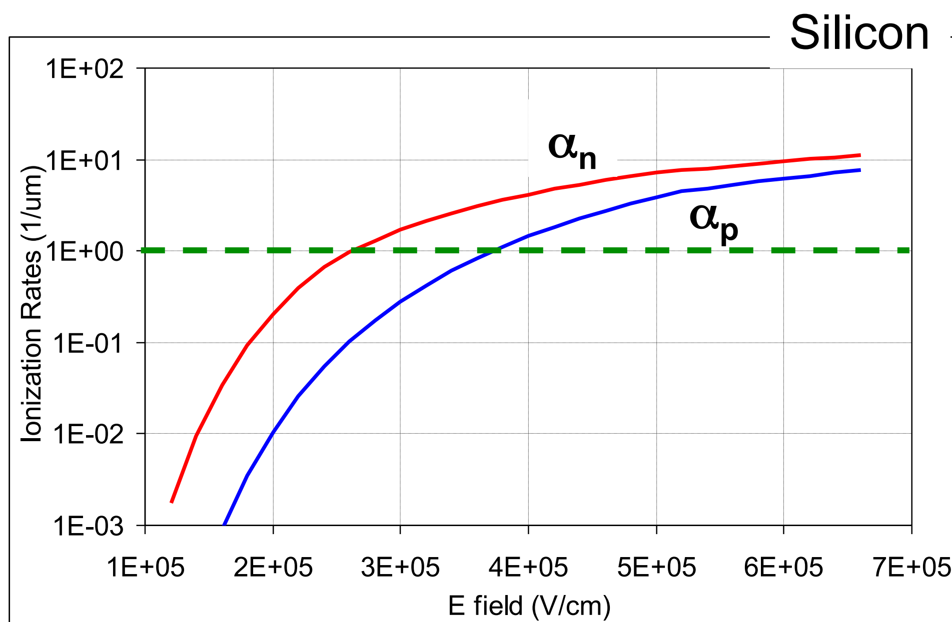

Ionization rates:
number of e-h pairs created by a carrier per unit distance travelled

Higher for electrons than for holes

Field ~2 – 3 x 10^5 V/cm required

Reverse current in a diode

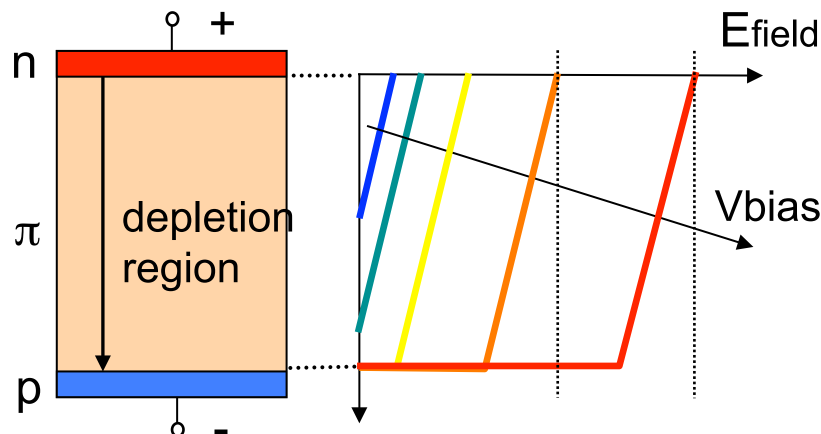

Low field region ($V<V_{APD}$)

Leakage current is mainly given by thermal generation in the depletion region:

$$I = q * G * W_{dep} = q * n_i * 1/\tau_g * W_{dep}$$

It reaches a constant value when fully depleted

High field region ($V>V_{APD}$)

Leakage current deviates from the expected constant value because some carriers "impact ionize"
A sort of "*GAIN*" could be defined

Very high field region ($V>V_{BD}$)

For even higher fields the phenomenon becomes uncontrolled and
the current rises indefinetely (in principle)
"*Infinite GAIN*"

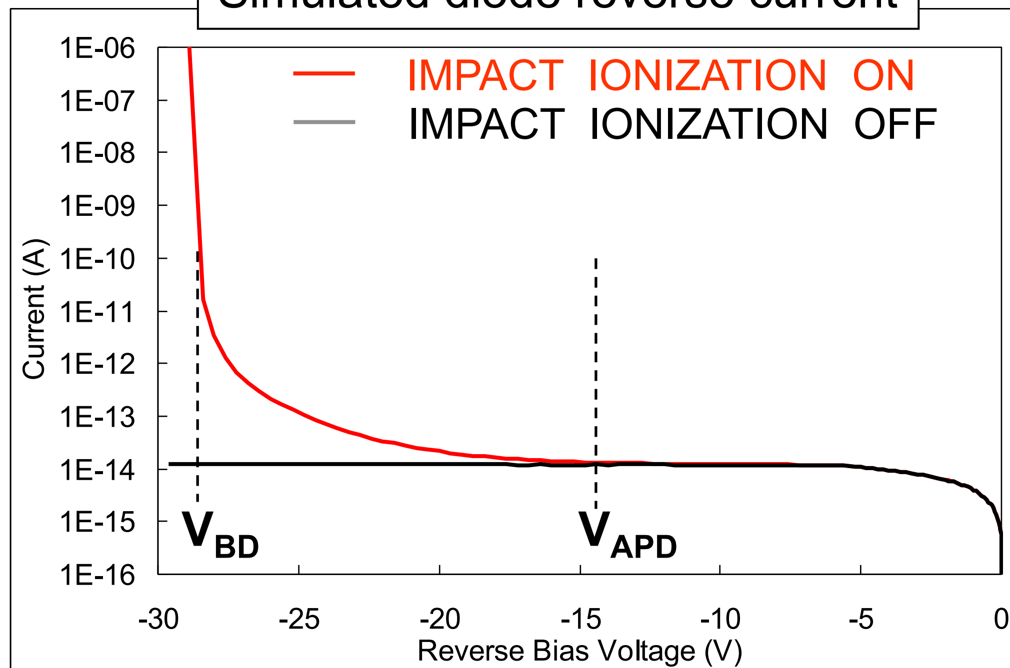

Avalanche PhotoDiode (APD)

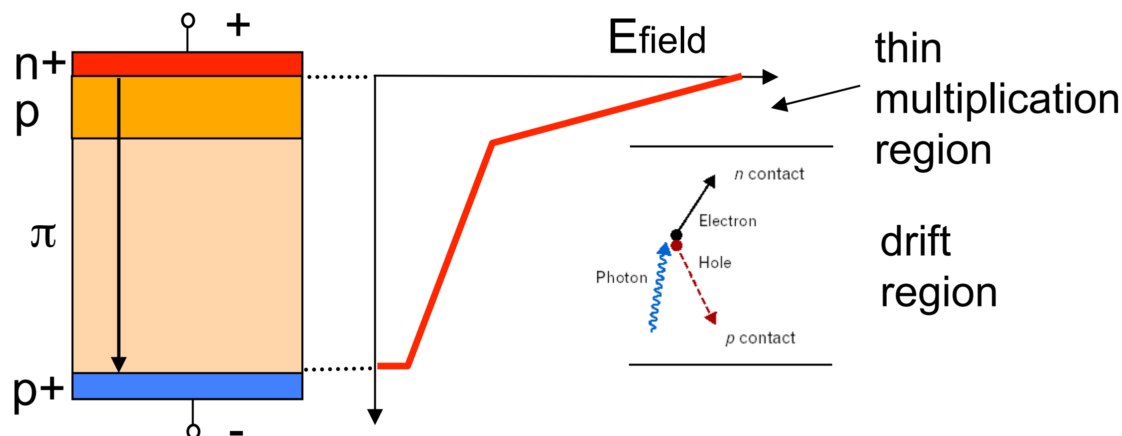

- Separated absorption and ionization regions

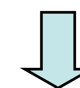

- All the electrons photo-generated in the drift region are multiplied (on average) by the same factor!

- $V < V_{APD}$
  => photodiode — 1 collected pair/generated pair
- $V_{APD} < V < V_{BD}$
  => APD — <M> (10-100) collected pairs/generated pairs
- $V > V_{BD}$
  => Geiger-mode APD — in principle ∞ collected pairs/generated pairs

GM-APD can detect even a single photon (SPAD)

Low Gain Avalanche Detector (LGAD)

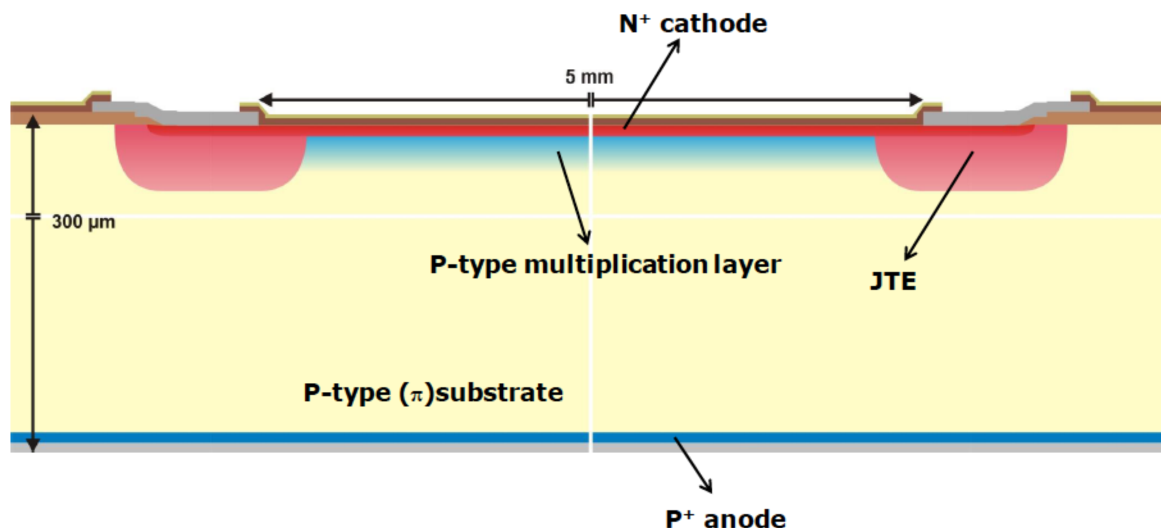

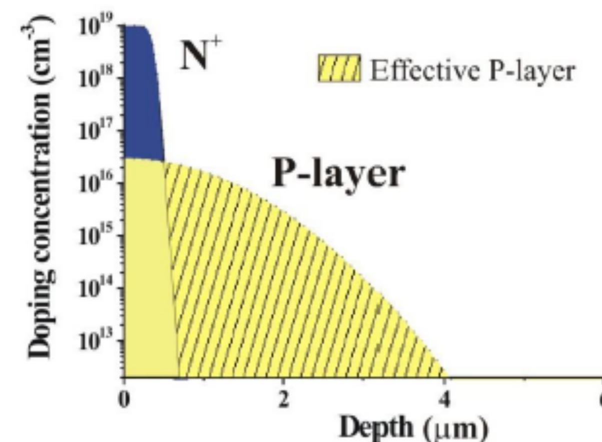

G. Pellegrini, et al., HSTD9 (2013)

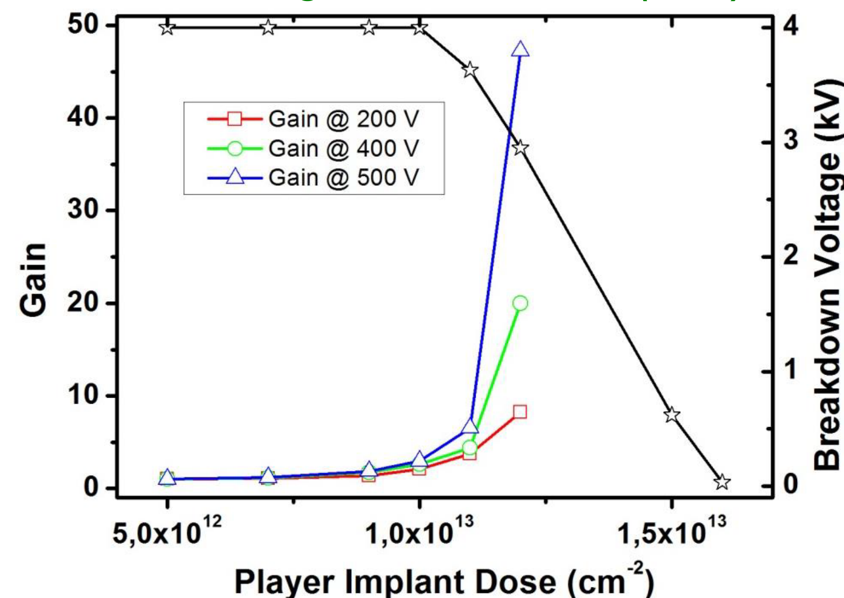

- APDs for ionizing particles
- Low gain for low excess noise
- Gain vs breakdown voltage trade-off
- High sensitivity to the implant dose of the multiplication layer …
- JTE to prevent from edge breakdown

LGAD performance

N. Cartiglia et al., 24th RD50 Meeting, 2014

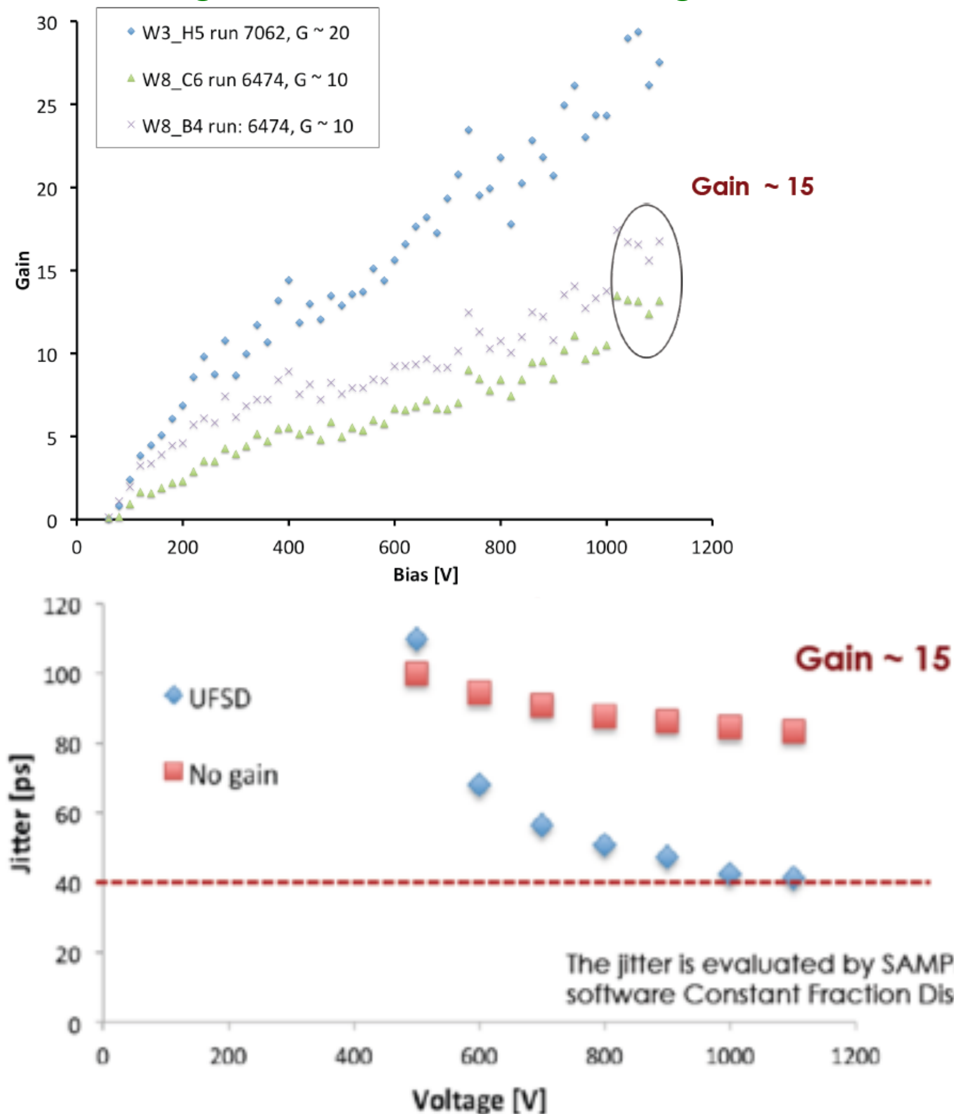

G. Kramberger et al., 24th RD50 Meeting, 2014

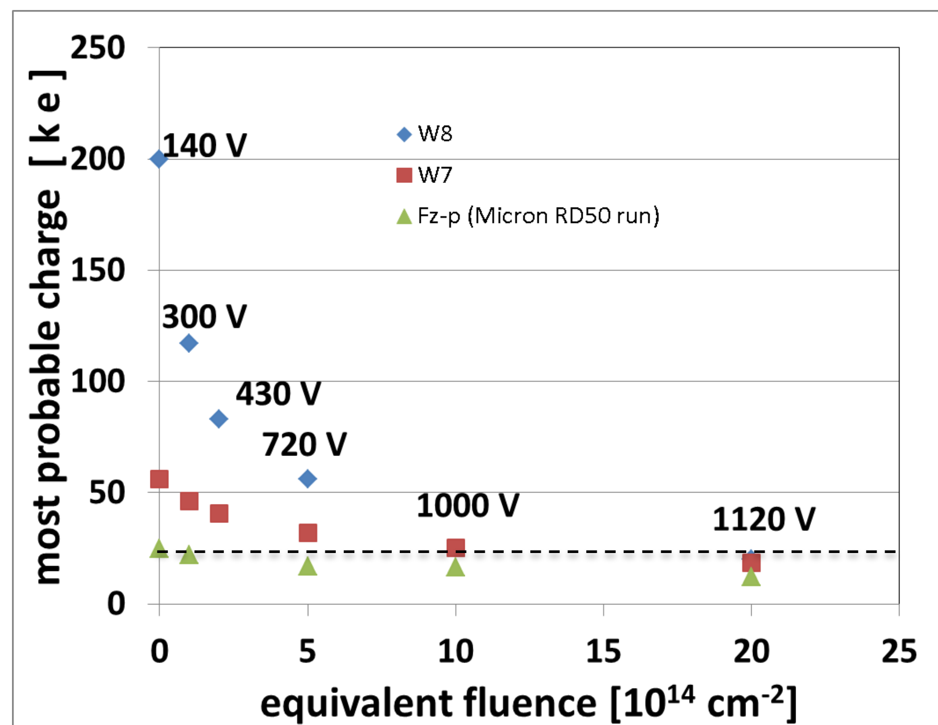

- It works well before irradiation
- It also improves timing res.
- But multiplication vanishes

after irradiation …

From pads to pixels: gain layer position/type

R. Arcidiacono, Detectors for Forward Physics at LHC, Elba 2014

Uniformity over large areas ?

SPAD based sensors ?

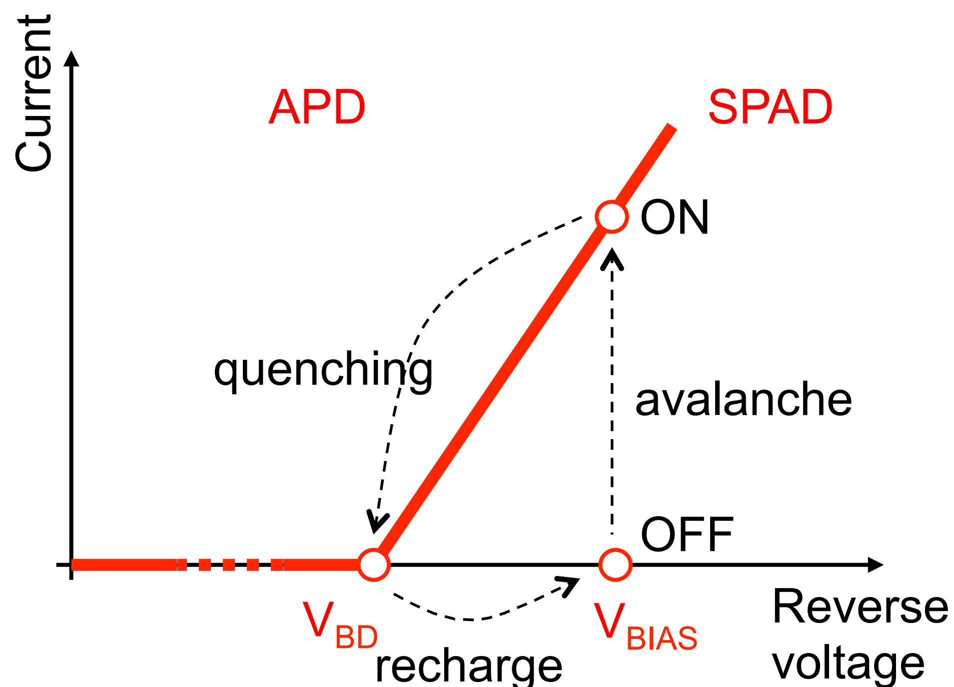

Main figures of merit

- Photon Detection Probability
- Timing resolution
- Primary noise:
  - dark counts
- Secondary noise:
  - Afterpulsing
  - optical cross-talk (for arrays)

S. Cova, et al., "Evolution and prospects for single photon avalanche diodes and quenching circuits". J. Modern Optics, 51 (2004) 1267

- Need for quenching/recharge mechanisms (→ dead time)
- Strong impact of excess voltage and temperature on most parameters

The silicon photomultiplier

SPADs are ON-OFF devices, i.e., they give no information on light intensity when irradiated with short (in time) bunches of photons

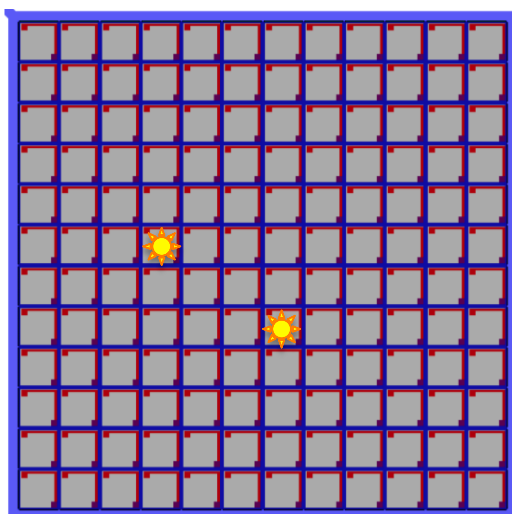

SiPM

first proposed by Golovin and Sadygov in the ’90s

A single SPAD is segmented in tiny micro SPADs connected in parallel.

Each element is independent and gives the same signal when fired by a photon

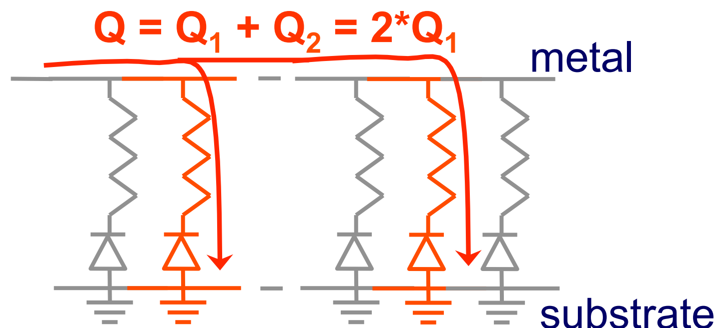

⇒ **output charge is proportional to the number of triggered cells that, for PDE=1, is the number of photons**

C. Piemonte et al., IEEE TNS 54 (2007) 236

SPAD in CMOS Technology

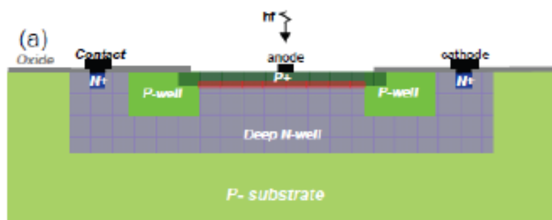

Goetzberger, 1963; Cova,1981; Kindt, 1994; custom
Rochas, 2002, CMOS 0.8; Niclass, 2007, CMOS 0.13;
Arbat, 2008, CMOS 0.35, Vilella 2009, CMOS 0.35

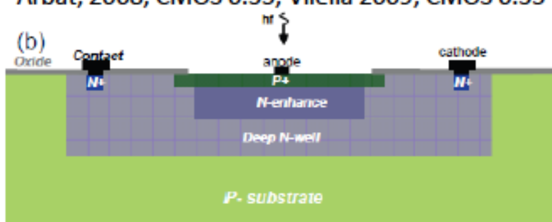

Petrillo, 1984; Ghioni, 1988, Lacaita, 1989, custom
Pancheri, 2007 CMOS 0.7

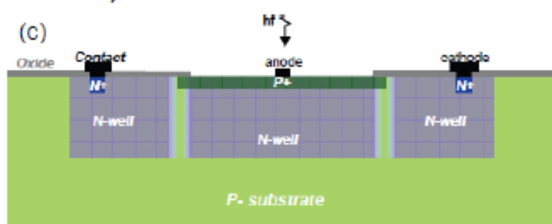

Pauchard, 2000; custom
Rochas, 2001, CMOS 0.8

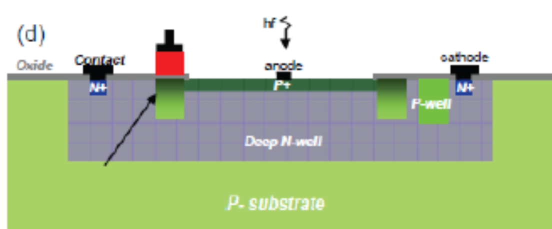

Rochas, 2003, CMOS 0.8; Xiao, 2007, CMOS 0.35

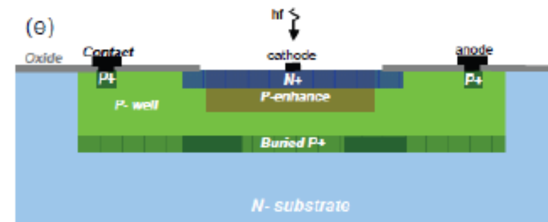

Cova, 1981; Ghioni, 1988, Lacaita, 1989; custom

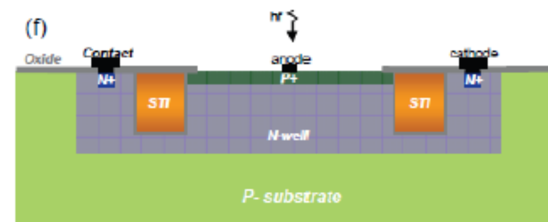

Finkelstein , 2006,CMOS 0.18; Hsu, 2009, CMOS 0.18;
Niclass, 2007, CMOS 0.13; Gersback, 2008, CMOS 0.13,
Arbat, 2008, CMOS 0.13

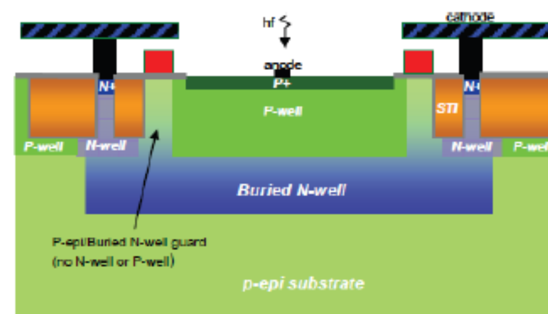

Richardson, 2009, CMOS 0.13, Webster, 2012, CMOS 0.09

G.-F. Dalla Betta et al., "Avalanche Photodiodes in Submicron CMOS Technologies for High-Sensitivity Imaging", in "Advances in Photodiodes", Intech House, 2011

SPAD based tracking sensors

- CMOS SPAD cells for charged particle detection
- Coincidence between vertically aligned cell pairs can dramatically reduce dark count rate
- Low material budget obtained with thinned sensors
- Intrinsically digital output → Simpler electronics
- On-chip electronics → reduced system complexity and power consumption

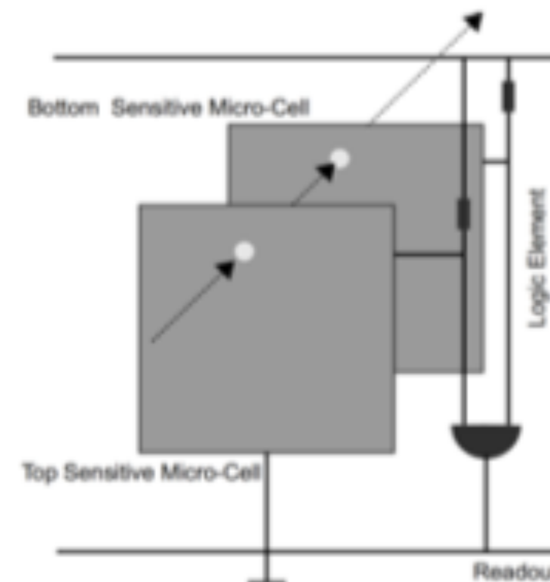

Questions to answer:

- Sensitivity: with very thin (~1μm) active volume, will SPADs detect all particles?
- Fill factor: is it possible to achieve a low geometrical inefficiency ?
- Noise: is DCR low enough (with standard CMOS process) ?
  what about optical cross-talk ?
- Radiation hardness ?

A. Dieguez, VERTEX 2013
P.S. Marrocchesi, et al., INFN APIX2 project

Conclusions

• It's still possible today to make p-n junction based radiation sensors more "intelligent" …

• 3D sensors have shown an impressive progress in the past few years and are now the most promising option for ultra radiation hard pixels

• Active edge sensors, from a side product of 3D, are now becoming a plus for many applications

• Avalanche based sensors, a standard in photon imaging, are being revisited for particle sensing: initial results are encouraging, lot of work still to be done.

Thank You

Back-up slides

ATLAS 3D common floor-plan

C. Da Via et. al.
NIMA 694 (2012), 321

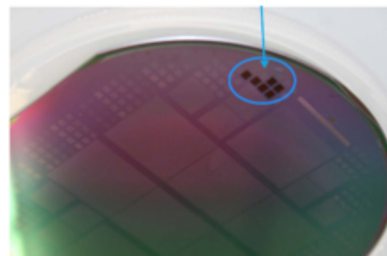

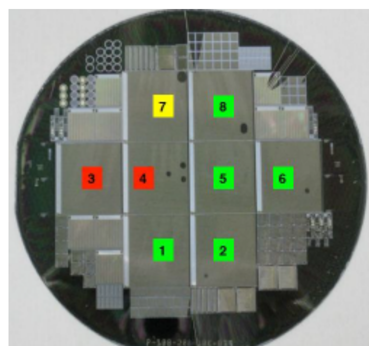

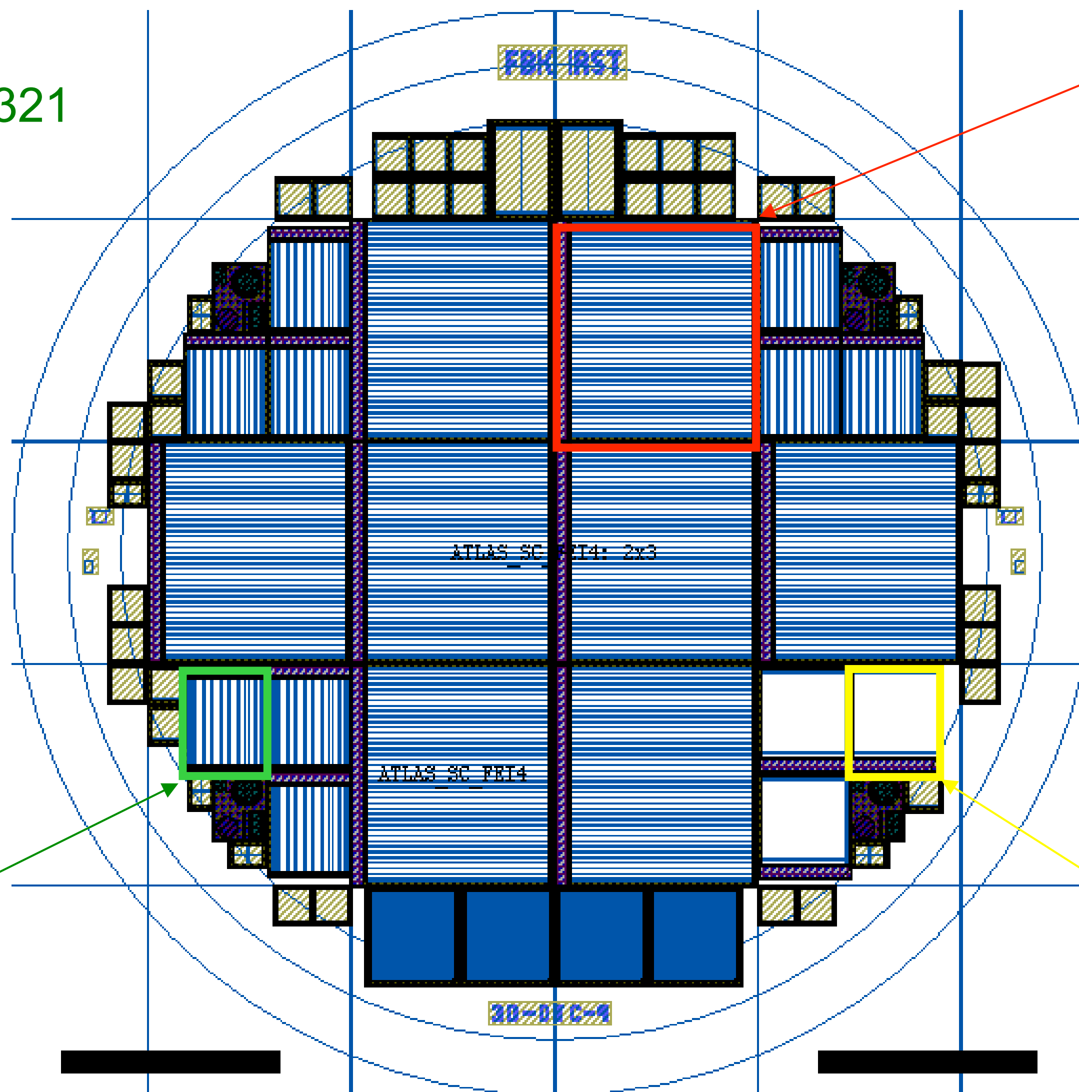

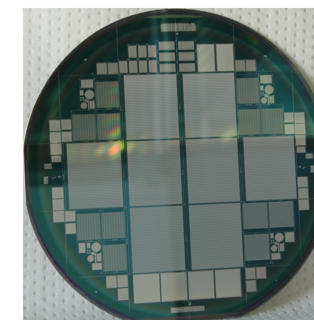

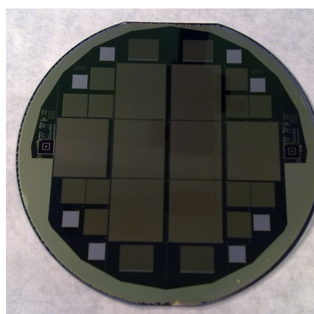

The ATLAS pixel Insertable B-Layer (IBL)

- Currently installed planar pixels have been designed for a fluence of ~1e15 n_{eq}/cm^2
- A new (4th) pixel layer will be inserted to improve the physics performance as close as 3.4 cm from the beam inside the existing pixel layers of the ATLAS experiment.
- The proximity to the interaction point requires new radiation hard technologies for both the sensors (6e15 n_{eq}/cm^2) and the front-end electronics (250 Mrad)
  - FE-I4, biggest pixel front-end chip (~4cm^2)
  - For 3D sensors, fabrication yield was a major concern …

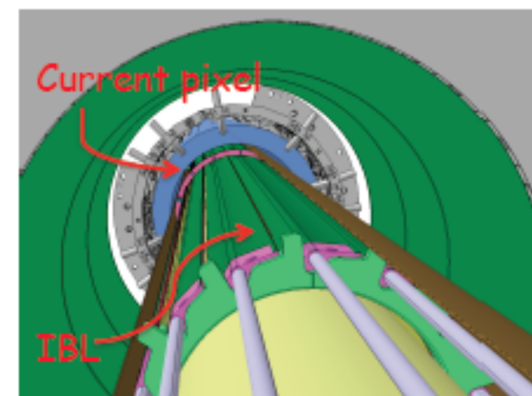

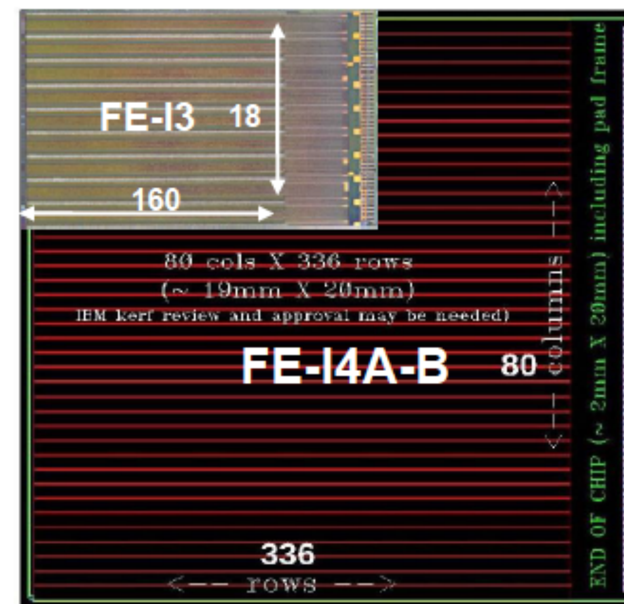

Specifications for ATLAS IBL 3D pixels

Main design specifications

- Two n^+ (read-out) columns per 250 μm pixel (2E)
- Inactive edge size along beam direction (Z) < 225 μm
- Sensor thickness = 230±15 μm

Wafer-level electrical tests

Parameter	Value
Operation temperature [T_{op}]	20 ÷ 24 °C
Depletion voltage [V_{depl}]	< 15 V
Operation voltage [V_{op}]	≥ V_{depl} + 10 V
Leakage current at operation voltage [$I(V_{op})$]	< 2 μa (full sensor) < 200 nA (guard ring)
Breakdown voltage [V_{bd}]	> 25 V
Leakage current "slope" [$I(V_{op}) / I(V_{op} - 5V)$]	< 2

On modules after irradiation at 5×10^{15} n_{eq} cm^{-2}

Parameter	Value
Operation temperature	- 15°C
Operation voltage	<180V
Power dissipation	< 60mW/cm²
Hit efficiency at 15 ° tilt angle	> 97%

Wafer-level electrical tests

The ATLAS IBL Collaboration, "Prototype ATLAS IBL Modules using the FE-I4A Front-End Readout Chip", JINST 7 (2012) P11010.

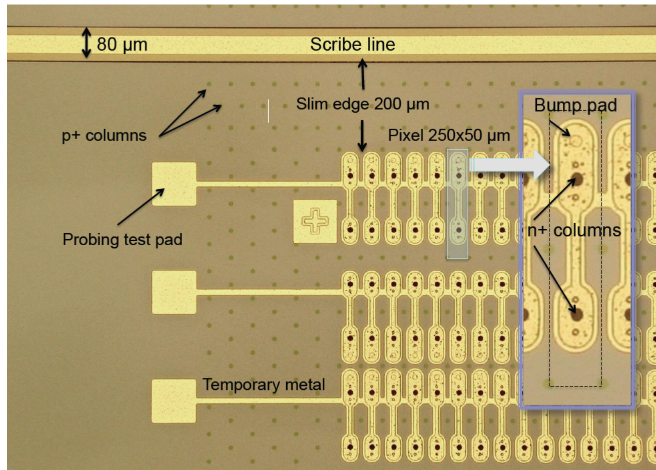

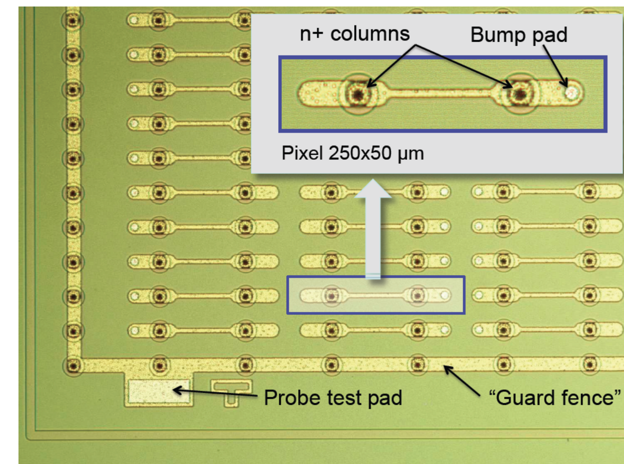

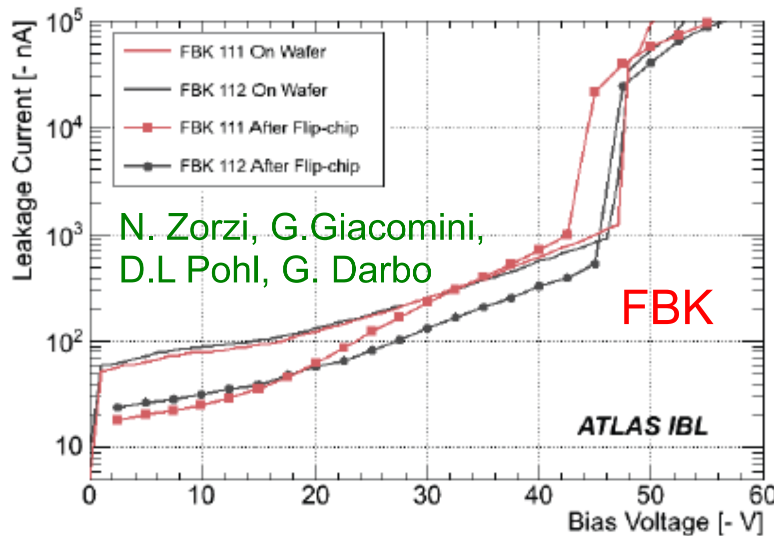

N. Zorzi, G.Giacomini, D.L Pohl, G. Darbo

FBK

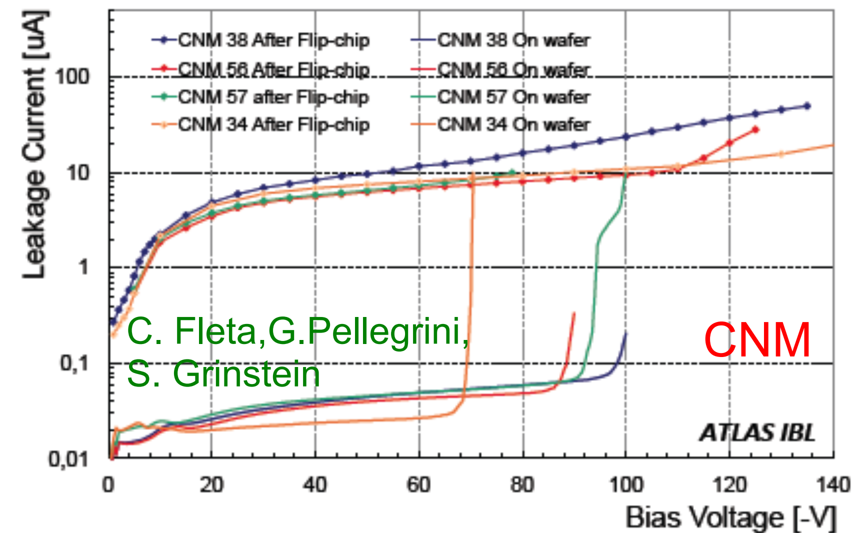

C. Fleta,G.Pellegrini, S. Grinstein

CNM

Edge efficiency in beam test

P. Grenier, S. Grinstein, Sh. Tsiskaridze

CNM34
p-irrad 5e15 n_{eq} cm^{-2}
Tilt 15°, 140V

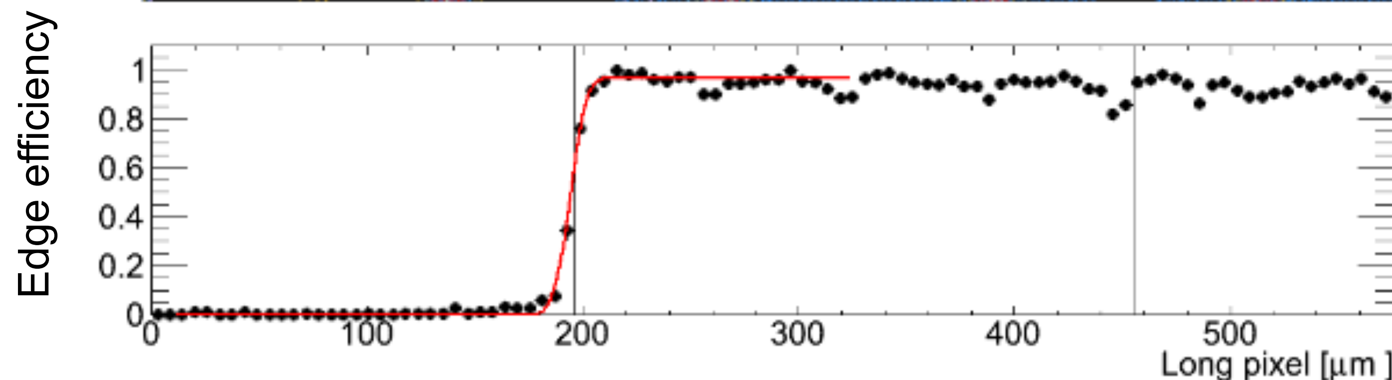

FBK90,
p-irrad 2e15 n_{eq} cm^{-2}
Tilt 15°, 60V

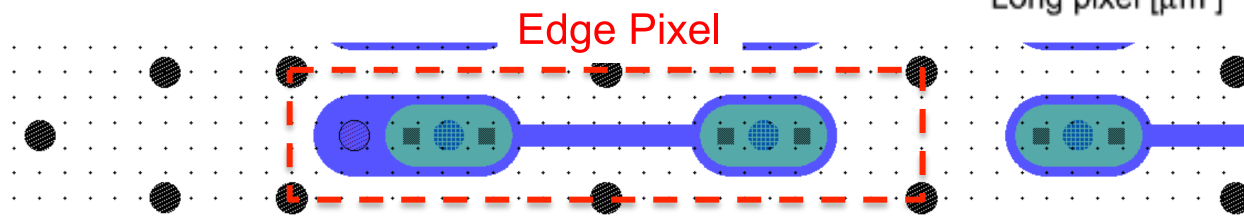

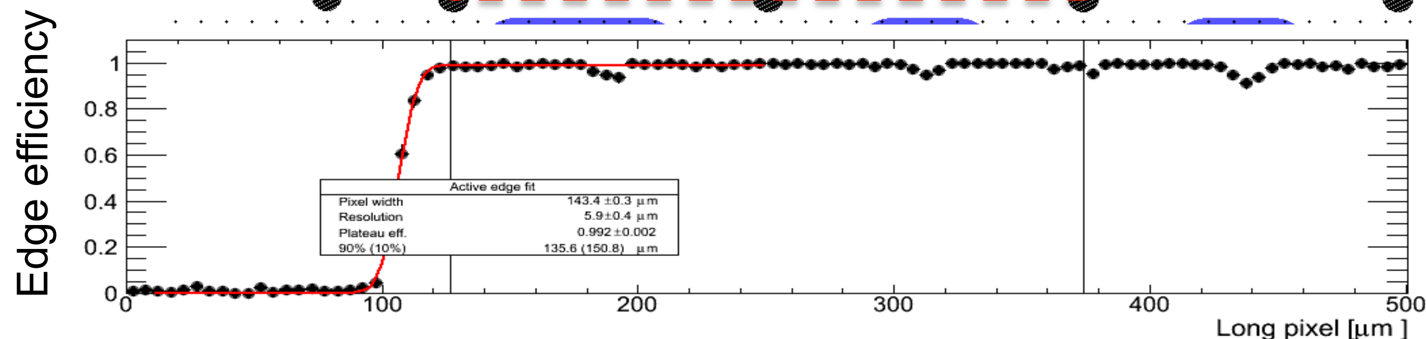

Summary of CERN beam tests results

The ATLAS IBL Collaboration, "Prototype ATLAS IBL Modules using the FE-I4A Front-End Readout Chip", JINST 7 (2012) P11010.

Sensor ID	Bias (V)	Tilt Angle °	Irrad.	Fluence (n_{eq}/cm^2)	Threshold (e-)	Hit Eff. (%)
CNM55	20	0	no	-	1600	99.6
FBK13	20	0	no	-	1500	98.8
CNM34	160	0	25 MeV protons	$5x10^{15}$	1500	98.1
CNM97	**140**	**15**	**25 MeV protons**	**$5x10^{15}$**	**1800**	**96.6**
CNM34	**160**	**15**	**25 MeV protons**	**$5x10^{15}$**	**1500**	**99.0**
CNM81	160	0	Reactor Neutrons	$5x10^{15}$	1500	97.5
FBK90	60	15	25 MeV protons	$2x10^{15}$	3200	99.2
FBK11	**140**	**15**	**25 MeV protons**	**$5x10^{15}$**	**2000**	**95.6**
FBK87	**160**	**15**	**25 MeV protons**	**$5x10^{15}$**	**1500**	**98.2**

DESY, 04/2012

Beam test results

The ATLAS IBL Collaboration, "Prototype ATLAS IBL Modules using the FE-I4A Front-End Readout Chip", JINST 7 (2012) P11010.

Irradiated 3D

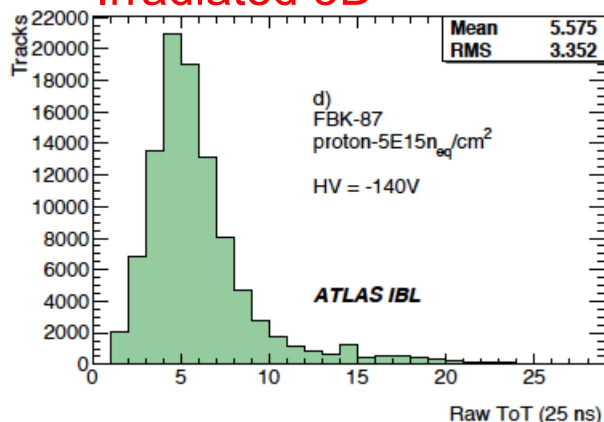

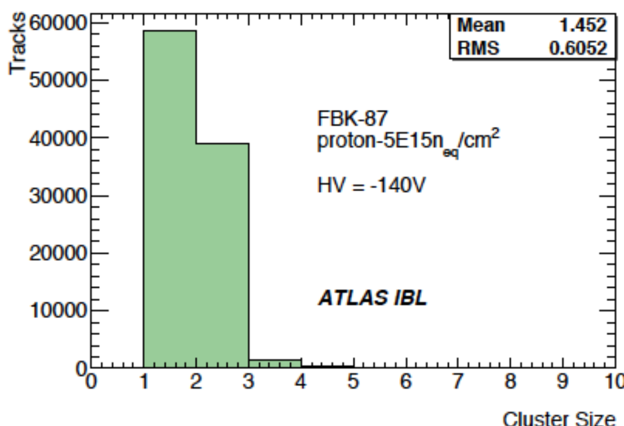

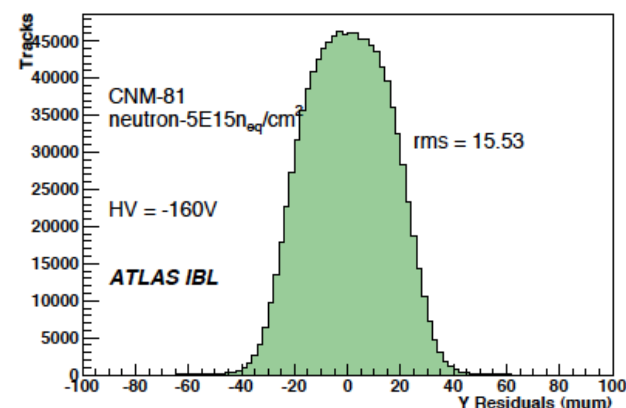

Irradiated planar

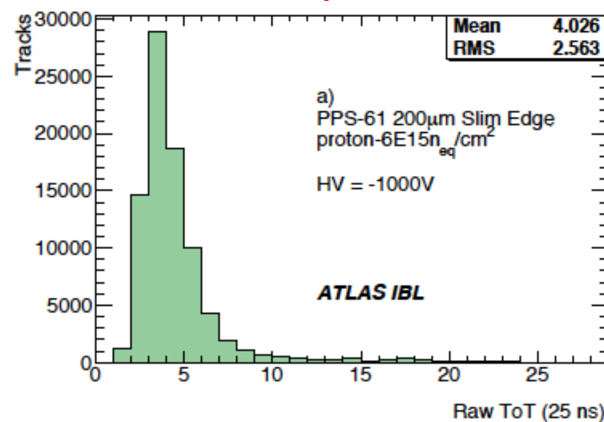

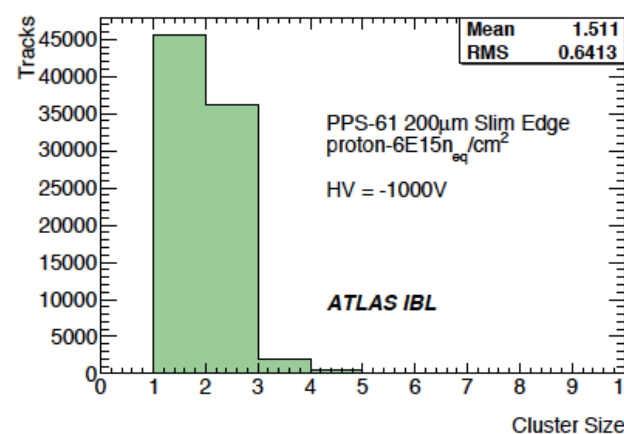

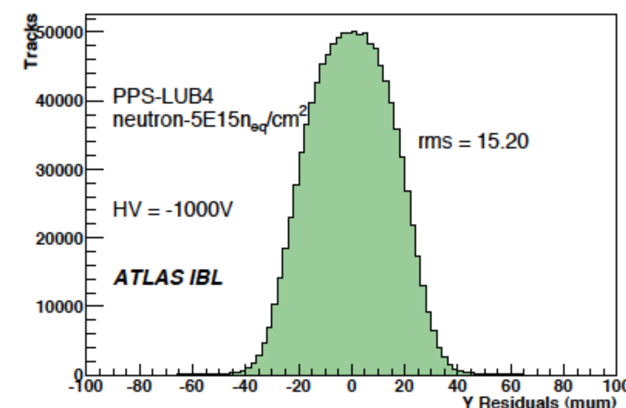

Looking at larger fluences with 3D strips

G.F. Dalla Betta et al, HSTD9 2013

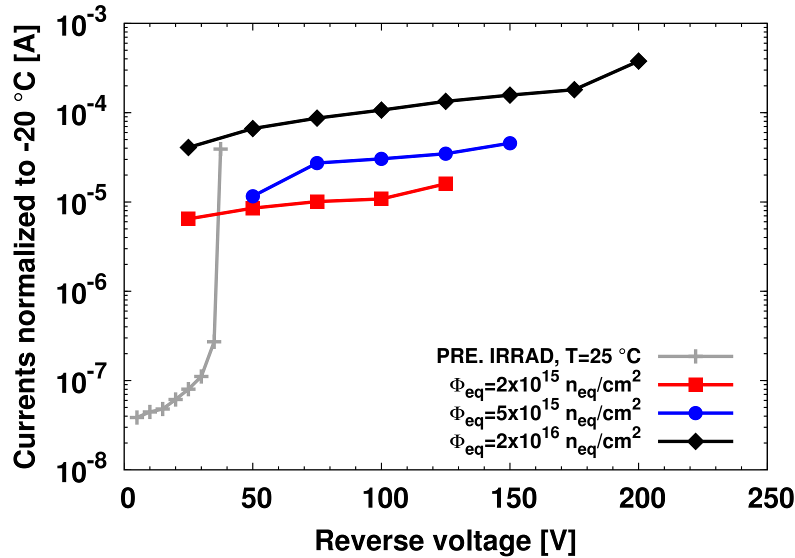

- Strip sensors from IBL prod. with ALIBAVA read-out
- Proton irradiation at KIT up to $2\times10^{16}\ n_{eq}/cm^2$
- Beta and laser tests performed in Freiburg
- Very good CCE, but clear saturation of the signal only for $2\times10^{15}\ n_{eq}/cm^2$
- For $2\times10^{16}\ n_{eq}/cm^2$ the bias voltage is not high enough to ensure uniform response …
- Need to improve breakdown voltage

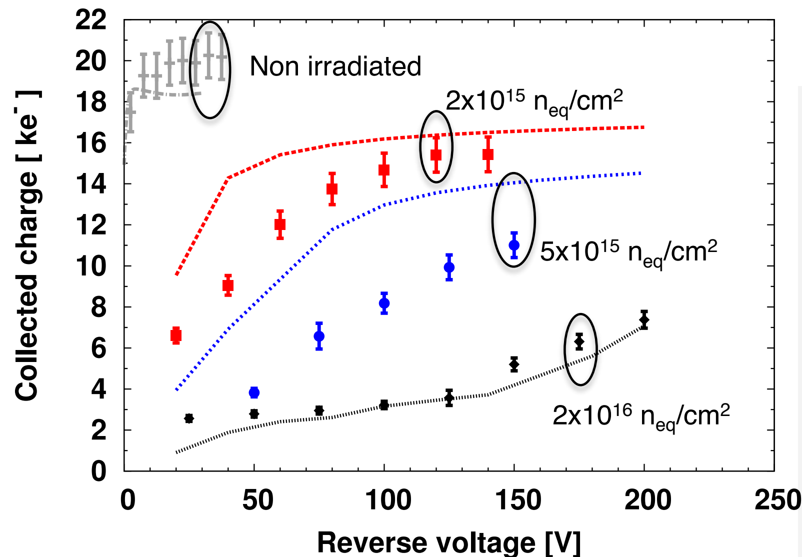

$2\times10^{15}\ n_{eq}/cm^2$, 120V

$2\times10^{16}\ n_{eq}/cm^2$, 150V

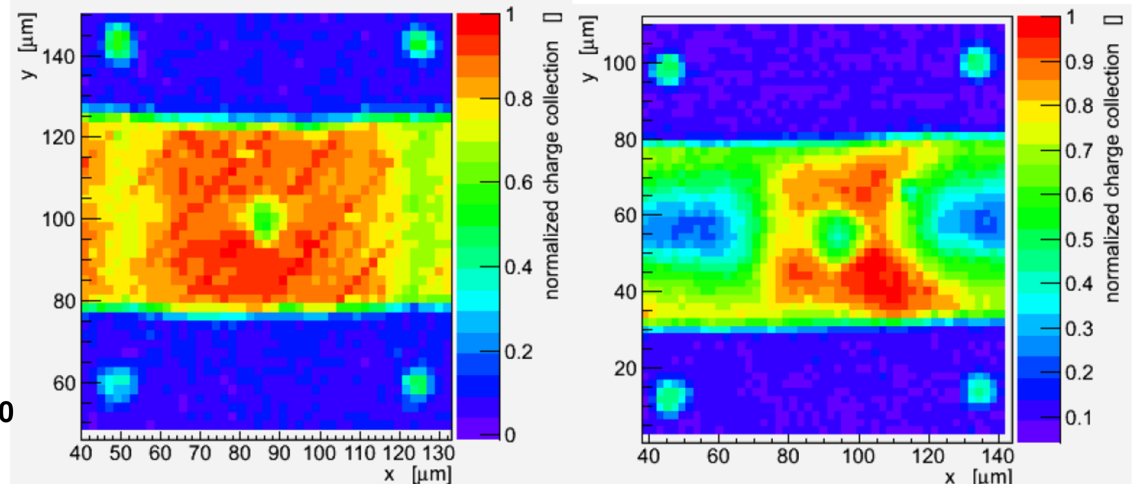

3D sensors for ATLAS Forward Physics

- AFP: detect very forward protons at 220m from IP
- Edge sensitivity and radiation hardness → 3D sensors
- But the irradiation pattern is very non-homogenous
  - Some regions of the sensor might require high bias voltage that other regions are not able to withstand due to breakdown

S. Grinstein, et al., NIMA 730 (2013) 28

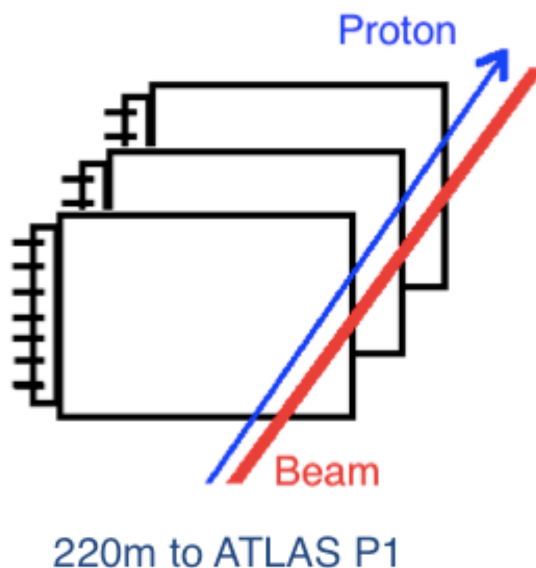

- Operated at 130V, -15°C, 0°
- Hit Efficiency: 98% after removing dead and noisy pixels

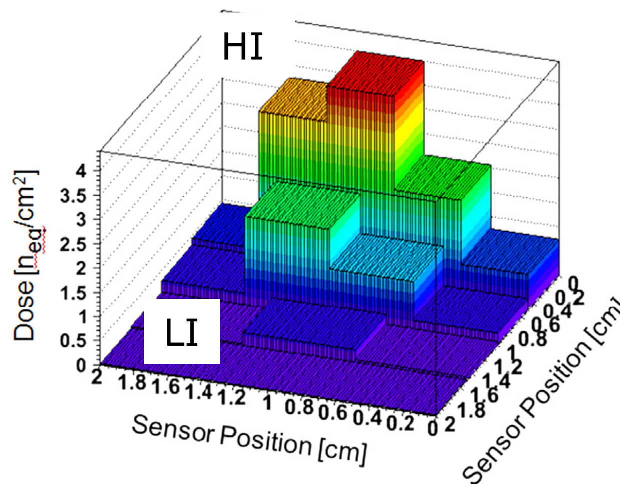

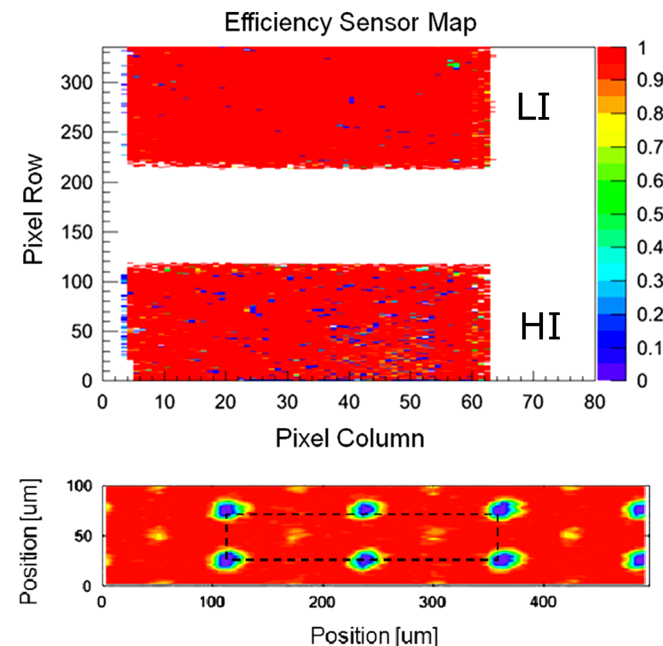

Proposed downscaled 3D Sensors

- Single-sided process with support wafer
- 100 to 150 μm active thickness
- 5 μm column diameter
- Two pixel layouts

50 x 50

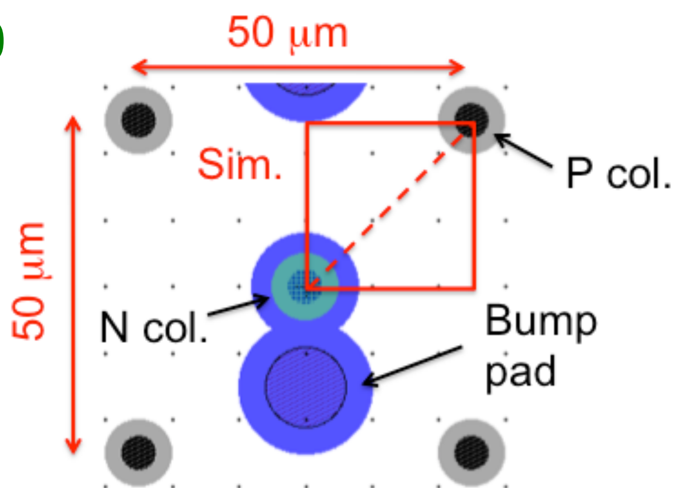

25 x 100

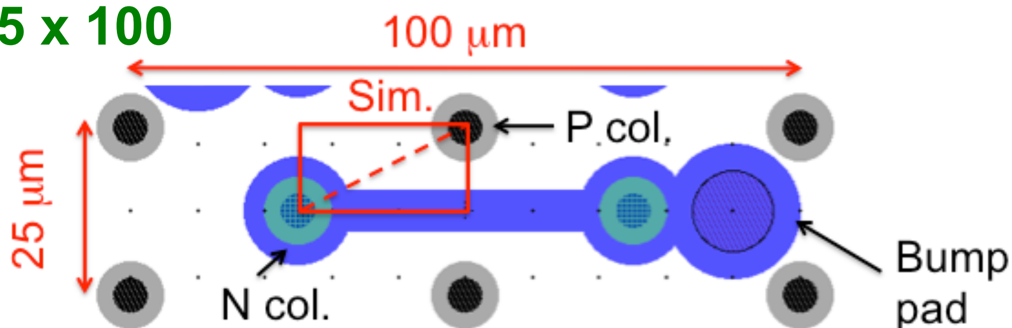

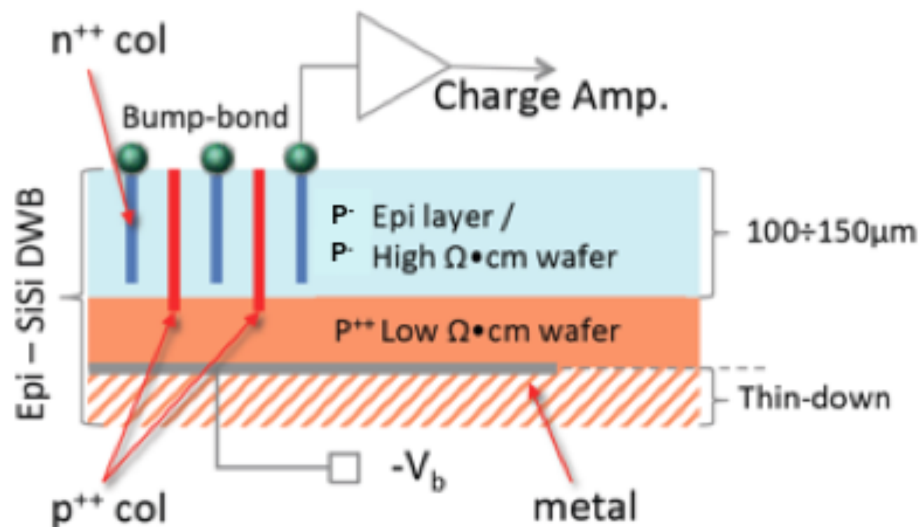

Pixel capacitance

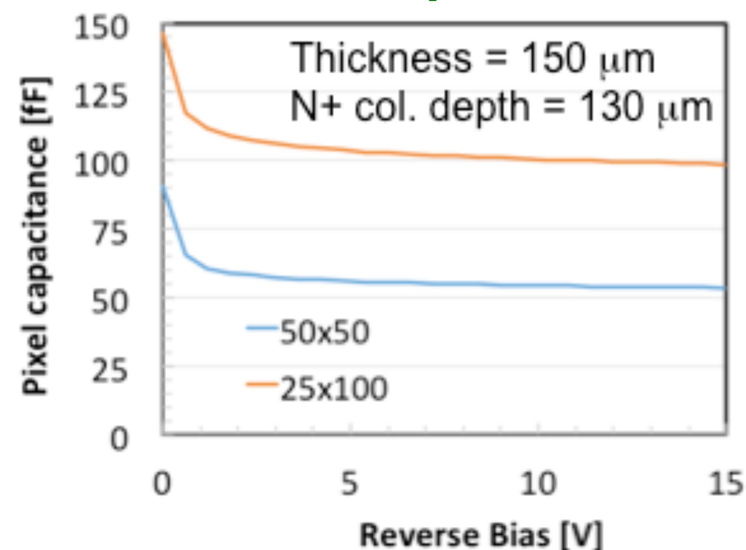

Thermal Neutron Detection with Semiconductors

- Thermal energy per particle is about 0.025 eV
- Need neutron reactive converter materials:

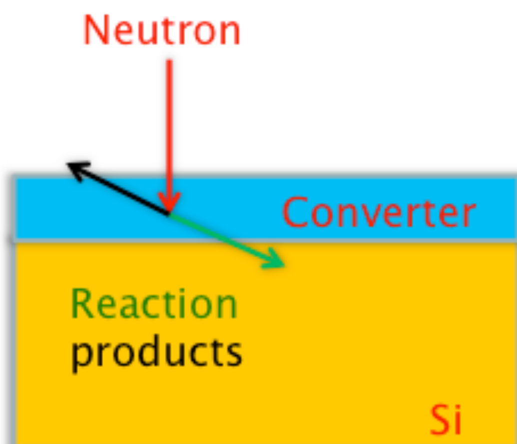

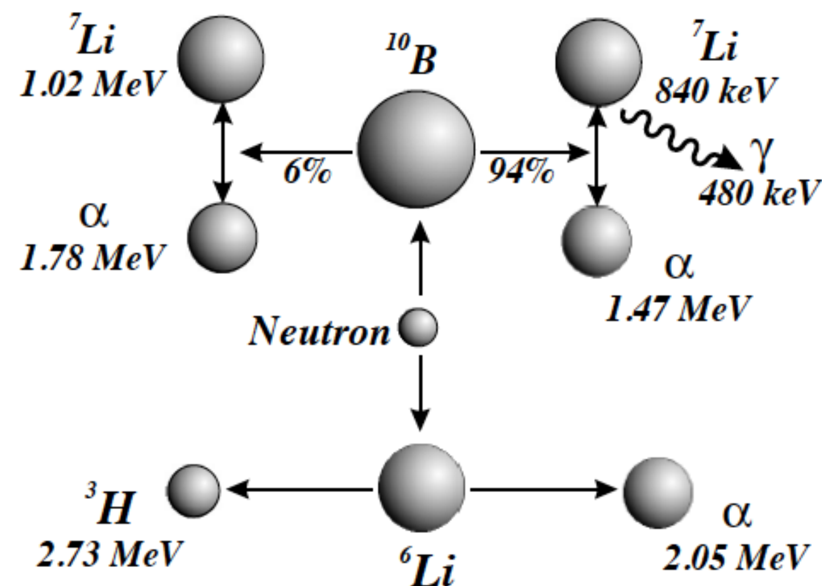

- With reference to ^{10}B converter:
  - 90% capture in 43 μm
  - Range of reaction products 2-5 μm
- Thickness trade-off for efficiency …
- Maximum reported absolute efficiency with planar sensors is 2-3%

3D hybrid neutron detectors

Higher efficiency (up to ~ 50%)

J. K. Shultis, D.S. McGregor, NIMA 606 (2009) 608

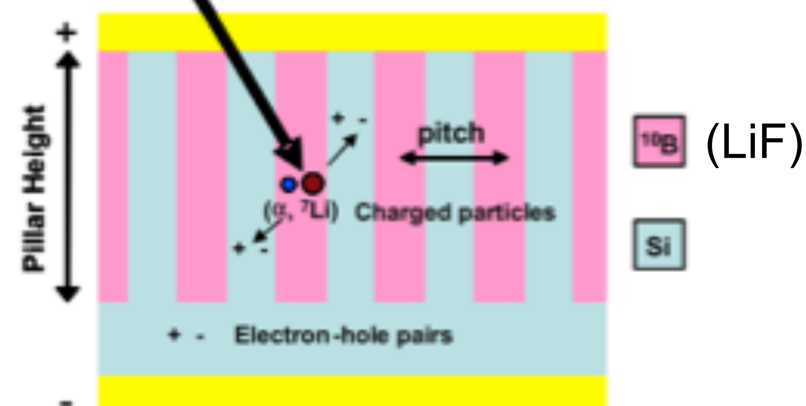

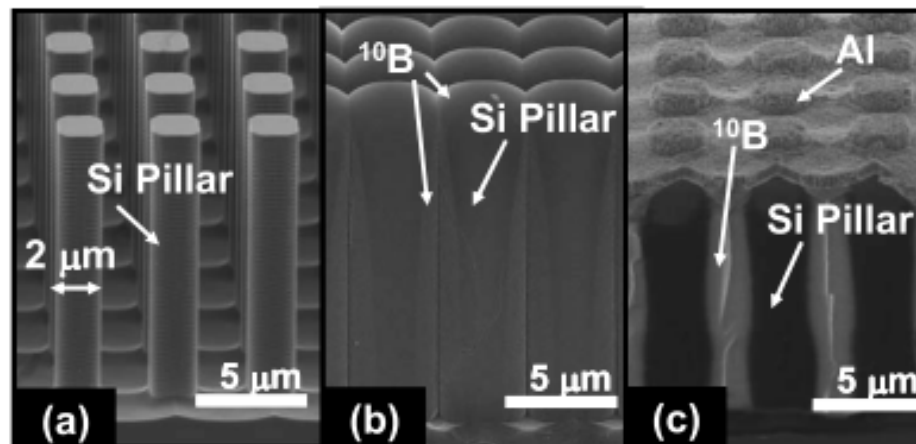

- **Different shapes and geometries**
- **Stacked detectors**

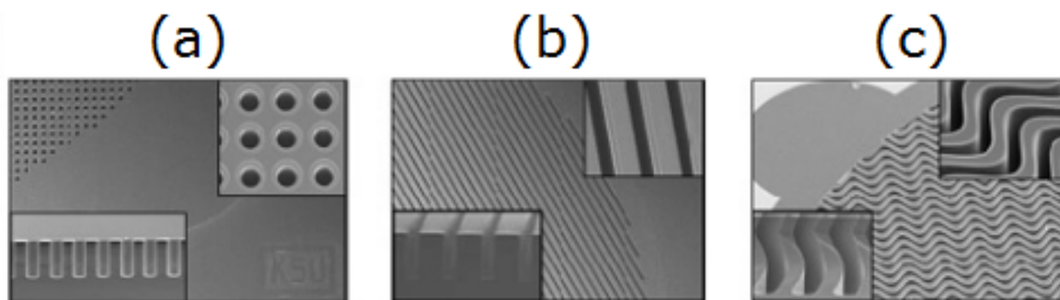

J. Uher et al., NIMA 576 (2007) 32
S. Bellinger et al., NIMA 652 (2011) 387
R. Shao et al. APL 102 (2013) 063505
Y. Danon et al., JINST 7 (2012) C03014

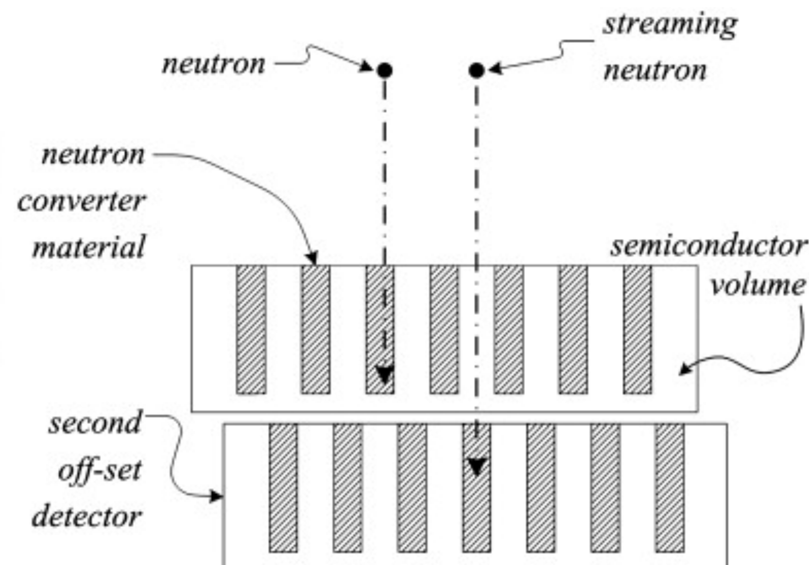

Also irradiated 3D sensors multiply …

- First evidence in 2008 on p-on-n 3D-DDTC strip sensors from FBK *A. Zoboli et. al., IEEE NSS 2008, N34-4*
- Comprehensive study by the Freiburg group on 3D-DDTC strip sensors from CNM *M. Koehler et. al., NIMA 659 (2011) 272*

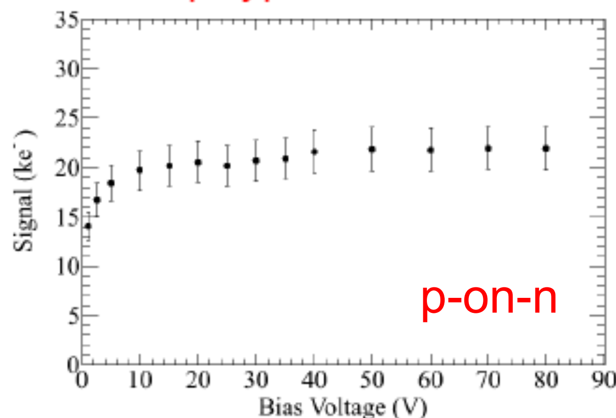

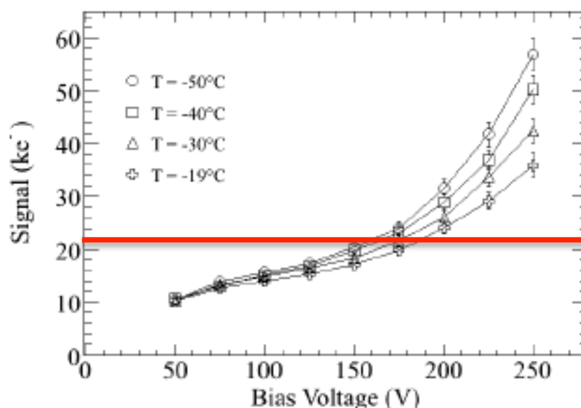

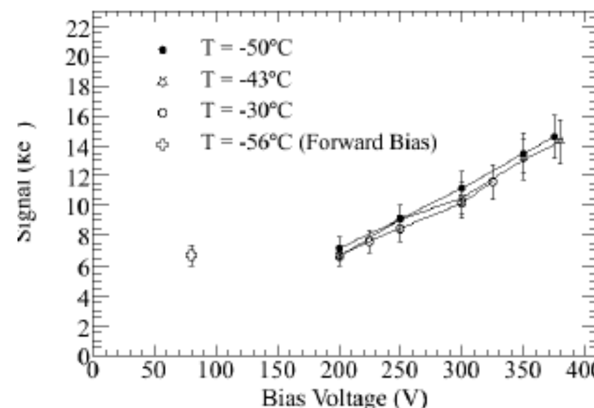

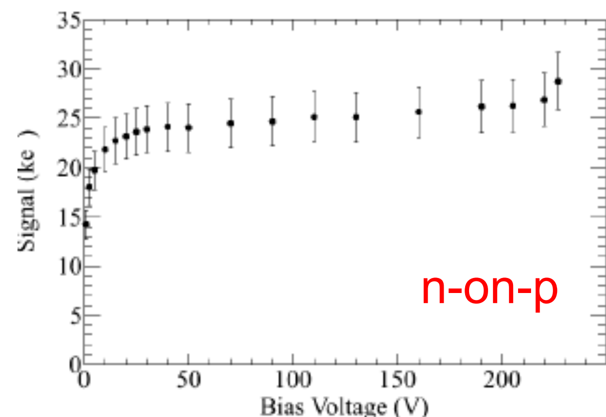

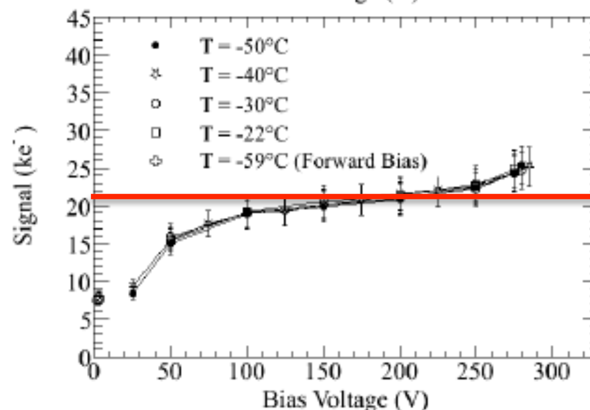

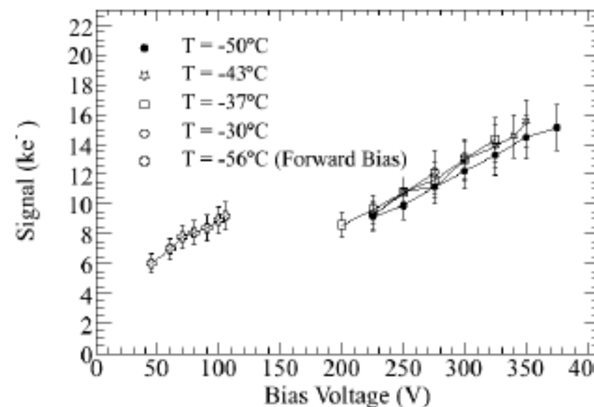

Before irradiation total charge 22ke-

$2x10^{15}$ n_{eq} cm^{-2} 22ke- at ~170V

$2x10^{16}$ n_{eq} cm^{-2} ~8ke-(15ke-) at 200V(350V)

Charge multiplication by design in thin 3D sensors

Exploiting high fields in thin 3D structures with small inter-electrode spacing

M. Povoli et. al., To be published